Stockholm University

Master Thesis

Degree Project in
Marine Geology 60 hp

Geophysical Mapping around Björkö Island in Lake Mälaren, South Central Sweden

Oscar Fransner

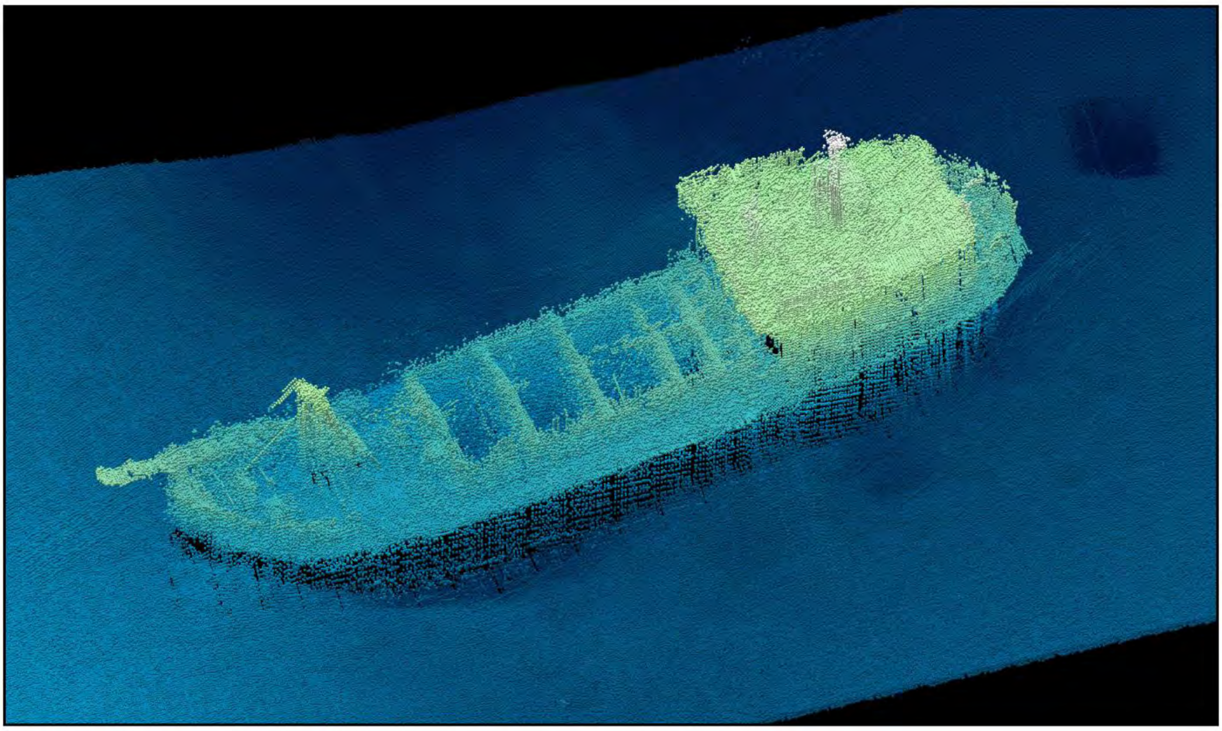

Stockholm 2013

Department of Geological Sciences
Stockholm University
SE-106 91 Stockholm

Geophysical Mapping around Björkö Island in Lake Mälaren, South central Sweden

Abstract

The former Viking settlement Birka is located on Björkö Island in Lake Mälaren, the third largest lake in Sweden. Birka is a well-known archeological site that onshore has been carefully examined. The lake floor of the waters surrounding the island has been less investigated but has a great potential to host not yet discovered archeological objects from this former hub for seafarers. Therefore, a geophysical survey including multibeam sonar mapping and subbottom profiling was carried out mainly along the shores of western Björkö Island. Processing and analysis of these collected data form the basis of this thesis. The main aims of this study are to produce a suite of geological maps and stratigraphic profiles that are used to geologically interpret the uppermost sediment stratigraphy and the bathymetry of the area. In addition, the processed data are investigated for archeological objects.

The result shows that the acoustic records of the sediment stratigraphy reaches back to glacial clay formed as a consequence of the retreat of the Late Weichselian ice sheet, and that the uppermost sediment units probably are from the time after the isolation of Lake Mälaren from the Baltic Sea. The bathymetry and backscatter results have revealed that this relatively shallow study area contains several objects that potentially could be of interest from an archeological point of view. These objects include several unidentified objects in the Björkö strait and two unregistered shipwrecks where ground truthing data need to be collected to determine their respective origin.

Keywords: Marine geosciences, geophysics, archeology, Birka, Mälaren, subbottom profiling, sediment stratigraphy, multibeam echosounder, backscatter, angular range analysis, shipwrecks.

Acknowledgments

First of all, I would like to thank my supervisor Martin Jakobsson who guided me through this project and who together with Roger Flood and Kerstin Lidén collected the data that is underlying this thesis. This work also greatly improved thanks to their comments and feedback. Tom Flodén, Richard Gyllencreutz and Francis Freire have been of greatest importance, always available with support and advice with all the new programs I encountered. The Birka group of the archeology department of Stockholm University has been valuable in the discussion of potential archeological artifacts in the datasets. Akkaneewut Chabangborn happily gave me illustrative support. I also want to thank my office mates Hamad Ali, Rooh Ullah and Martina Potucek for the supportive attitude we had.

Table of Contents

1. Introduction

Birka is located on Björkö in Lake Mälaren, in South central Sweden. To understand how Björkö developed, knowledge about the Post-Glacial development of the Baltic Sea is essential.

During the last 12600 cal yr BP, the modern Baltic Sea has gone through several environmental stages which were influenced by the northward retreat of the Late Weichselian ice sheet from its front position in south central Sweden. Due to this event, an ice lake formed in the Baltic basin. This ice lake is called the Baltic Ice Lake. The Baltic Ice Lake existed from 12600 to 11570 cal yr BP (Andrén et al., 2000) and is the initial stage of the modern Baltic Sea (Lundqvist, 2004). The ice lake grew on the expense of the retreating ice sheet which also fed the lake with melt water and glaciolacustrine sediments (Björck, 1995). These sediments mainly consisted of clays, where the varved clay type was most prominent close to the ice margin while non-varved clays formed in distal areas (Ignatius, 1958).

In the beginning of the Baltic Ice Lake stage, the accumulating melt water found its outflow to the North Sea through Öresund. Due to the increasing isostasy this outflow was eventually dammed. The growing Baltic Ice Lake then rose above the sea level due to the accumulating water masses from the retreating Late Weichselian ice sheet (Björck, 1995). Eventually, the northward retreat of the Late Weichselian ice sheet opened up a new outflow for the Baltic Ice Lake, which led to a rapid decrease in water volume of the Baltic Ice Lake. The outflow was located in between the northern part of Mount Billingen and the margin of the retreating Late Weichselian ice sheet in south central Sweden. The outflow was redammed during the Younger Dryas cool period due to a temporal regrowth of the Late Weichselian ice sheet. A second, apparently more dramatic drainage happened in the same place as the previous one at the end of the Younger Dryas cool period. This drainage took place in between 11700 and 11600 cal yr BP which led to a reconnection in between the Baltic Ice Lake and the North Sea (Björck, 2011).

After the second drainage and the connection to the North Sea, the Baltic Ice Lake could not recover due to a warmer climate and a faster northward retreat of the ice sheet. Instead the next stage of the Baltic basin formed, which is called the Yoldia Sea (Björck, 1995). This stage existed from 11600 to 10700 cal yr BP, and is characterized by a slow increase of brackish water in the Baltic basin due to the inflow of marine water from the connection to the sea (Björck, 2011). Varved clays were still the dominating sediment type close to the ice sheet margin, but further away the varves got more diffuse (Brunnberg, 1988). Due to the increased melting the sedimentation rate at this time was faster than during the Baltic Ice Lake stage (Björck, 1995). The removal of ice from melting also initiated an isostatical uplift of the land areas that earlier were depressed by the overlying ice sheet. The latter factor is the main cause why the straits that connected the Yoldia Sea to the North Sea gradually became shallower, which once again led to a disconnection in between the Baltic basin and the North Sea (Björck, 1995; Björk, 2011).

This disconnection marks the beginning of the Ancylus Lake, which is the third of the stages that the modern Baltic Sea has gone through. The Ancylus Lake existed from 10700 to 9800 cal yr BP and was a fresh water lake with low primary productivity that got its water supply exclusively from the melting Late Weichselian ice sheet. The dominating sediment type was therefore increasingly glacially influenced and organic-poor the closer to the retreating ice margin in the North (Andrén et al., 2011).

The fourth stage of the Baltic basin, named the Littorina Sea gradually took over about 9800 cal yr BP. The main cause behind this event is probably the flooding of the Öresund Strait, which in turn happened as a consequence of a ceased isostasy in this area together with a relatively rapid increase in global sea level due to the melting ice sheets in both the North - and the South Poles (Andrén et al., 2011). The Littorina Sea is characterized by its brackish water and relatively high primary productivity, which is displayed as organic rich sediments and anoxic bottom conditions. The Littorina Sea had a higher salinity concentration than the modern Baltic Sea, which is the major difference in between these two stages. The modern Baltic Sea took place about 3000 years ago (Björck et al., 1996; Björck 2011).

The interaction in between the eustasy and isostasy after the retreat of the Late Weichselian ice sheet has proven to have had a great impact in the sharpening of the modern geography around the Baltic Sea. For example, the formation of several islands took place in the Mälaren area (Nationalencyklopedin; SGU, 2012-05-08). One of these islands is named Björkö, and is today situated in Lake Mälaren about 30 kilometers west of Stockholm (Harrison, 2009) (fig. 1.1).

On Björkö, when Mälaren still was connected to the Baltic Sea, the Viking settlement and trading port of Birka was founded in the middle of the 8th century (fig. 1.1). The location of the island was strategic and opened up possibilities for long distance trading, which became the major contribution to the wealth of the Birka settlement. Eventually, Birka expanded to become the first urban community of Sweden, with an estimated population of 500 to 1000 inhabitants (Harrison, 2009). The activity in Birka was thriving but lasted only for a short time period. About 200 years after its establishment, Birka ceases after a violent attack on its fort (Holmquist-Olausson, 2002). It is also possible that the isostasy contributed to why Birka never was rebuilt since it made the connections between Lake Mälaren and the Baltic Sea too shallow to use as sailing routes (Risberg et al, 2002). In between 1000 and 1300 AD, the isostasy reached a point when Lake Mälaren was formed due to the disconnection from the Baltic Sea (Risberg et al., 2002). This implies that Lake Mälaren is relatively young, and is today the third biggest lake in Sweden with its total area of 1600 km^2 (Nationalencyklopedin; SGU, 2012-05-08).

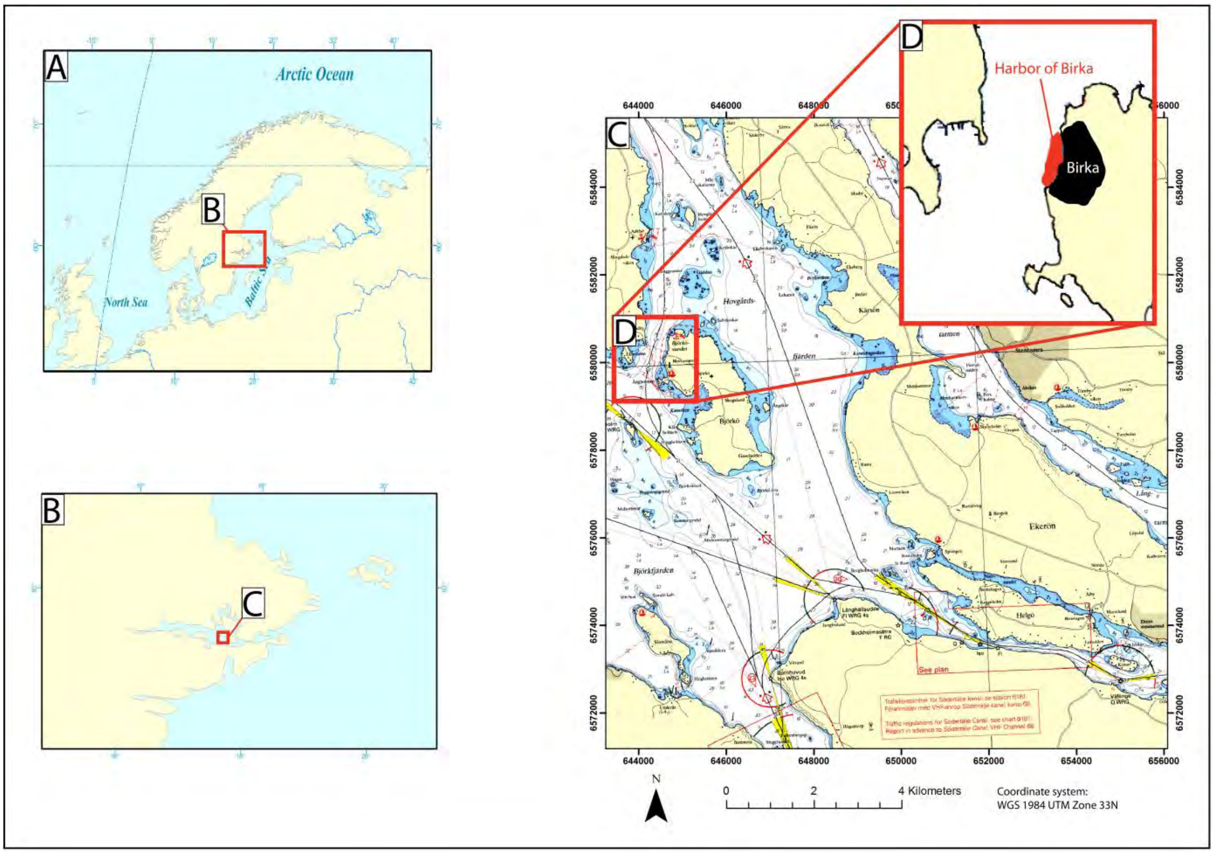

Figure 1.1. Northern Europe (A), Eastern Sweden (B) and a detailed navigational chart of the study area around Björkö (C). The location of Birka on the island of Björkö is marked with a red box (D). Basemap A and B are from Arc Map while C and D are from Sjöfartsverket navigational chart: Mälaren – Östra delen.

Original remains on Björkö consist of Viking tombs covered by a cultural soil horizon called "the black soil" (Harrison, 2009). This soil layer, which covers most of the area that once was Birka, mostly consists of remains from human activities, such as cleaning of latrines and ditches, cutting of vegetation, ash, livestock dung and bones. The soil horizon is therefore important because it partly indicates how the Vikings of Birka lived and what they ate. The black soil is to some extension even found on the lake bottom outside the former harbor of Birka (Risberg et al, 2002). In addition to the black soil, the harbor area also has remains of a water palisade. This palisade is suggested to have been constructed by the Vikings to protect Birka from unwanted ships (Risberg et al, 2002; Harrison, 2009).

In May 2011, the Department of Geological Sciences from Stockholm University carried out a geophysical survey offshore Björkö using their Kongsberg EM2040 multibeam sonar and Meridata MD500 penetrating echo sounder. The two instruments were run separately and do therefore not follow the exact same survey lines (figs 1.2a and b). Still they had the same focus, namely "Björkösundet". This is the strait in between Björkö and Adelsö where the potential of locating archeological objects are relatively high since Birka and its harbor were located here. It should also be mentioned that the group of survey lines inside the black ellipse (fig. 1.2a) are from the patch test of the underlying survey, and will not further be considered.

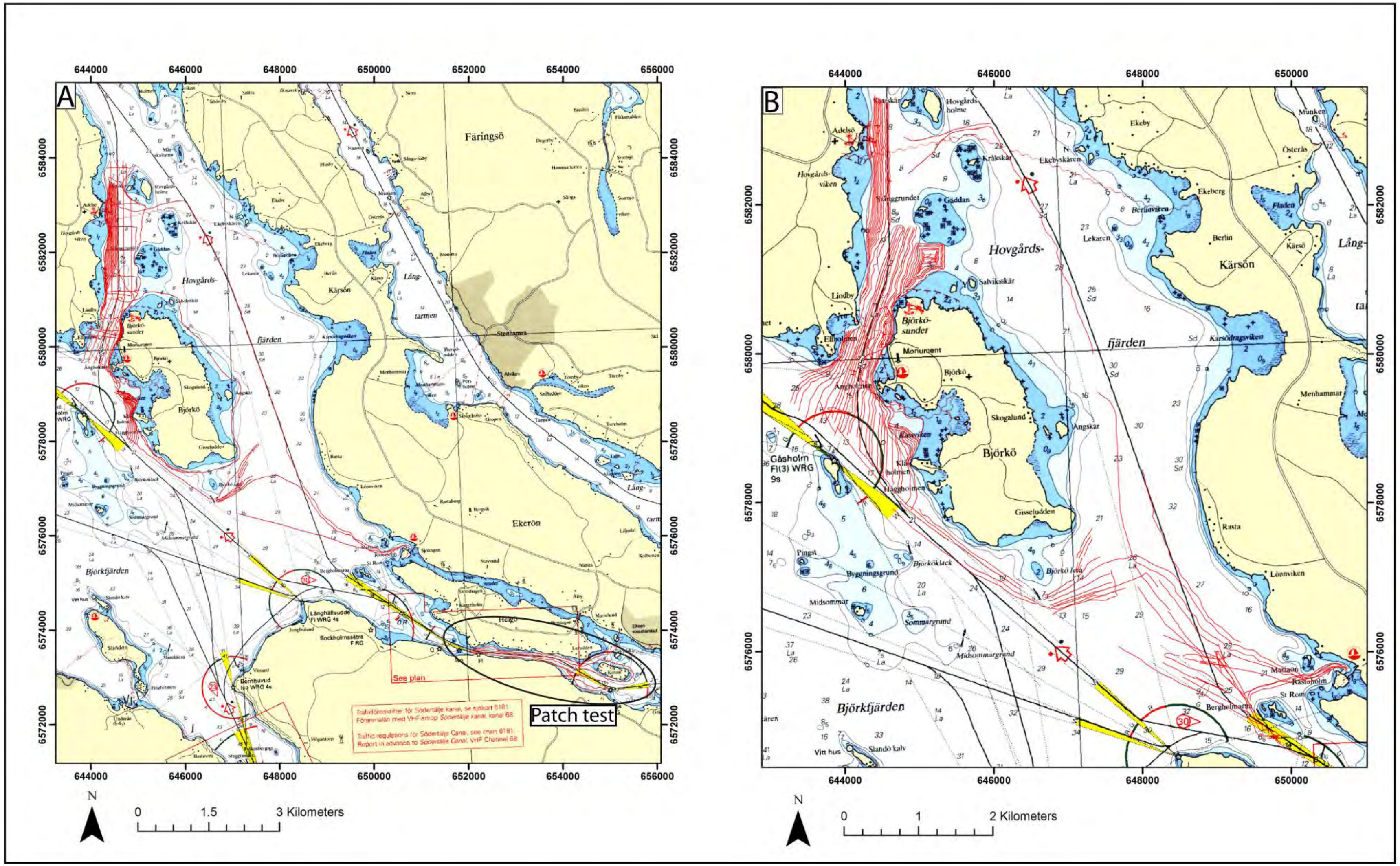

Figure 1.2. Survey lines in red for the subbottom profiler (A) and multibeam sonar (B). Focus for the two surveys were put on Björkösundet – the strait in between Björkö and Adelsö where the potential to find archeological artifacts are higher. Basemaps are from Sjöfartsverket navigational chart: Mälaren – Östra delen.

In this thesis, the geophysical mapping data collected during the mentioned survey have been processed and analyzed for two main purposes:

1) Interpretation of the uppermost few meters of the sediment stratigraphy of the Björkö Strait, where the distribution and volume of "the black soil" is addressed.

2) Production of a bathymetric map of the strait where features that may be of geologic or anthropogenic origin are highlighted and described with associated backscatter data.

The features on the lake floor identified with the multibeam sonar are both of geological and anthropogenic origin, where the latter group potentially can be of archeological value. What obstructs the acoustic classification of potential archeological objects is the fact that the area offshore Björkö in modern times often has been used as a dump, where anything from tiled stoves to barge vessels have been thrown away (Lidén, personal communication). For this reason it is hard to directly establish whether identified objects of likely anthropogenic origin are of archeological interest without additional ground truth data, i.e. diving.

Even if the anthropogenic objects are not of any archeological value, they can still be worth to examine from an environmental point of view. In particular this is true for shipwrecks due to degradation of potentially hazardous fuel tanks and cargo storages. Therefore, all modern shipwrecks should be classified as "potential polluting shipwrecks" (PPSWs) (Masetti and Calder, 2012). To examine and register shipwrecks is even more important in closed basins and lakes, where the impact of leaking chemicals are greater than in open oceans (Svensson, 2010).

All the objects that have been found in the data sets during this work are therefore presented in this thesis regardless their shape, size and location. The intention is to identify features that may be of interest for further ground truthing, and be inclusive rather than exclusive. In Appendix 8.2 all the objects of interest have been listed together with their coordinates (WGS 84 UTM zone 33 N).

2. Study area

The study area of this thesis is located in Lake Mälaren offshore the island of Björkö (fig. 1.1). The general bathymetry of the area shows that the relatively shallow Björkö strait in between Björkö and Adelsö ends with a natural threshold parallel to Adelsö in North-South direction immediate above Björkö. This threshold acts as a natural barrier in between the Björkö strait and “Hovgårdsfjärden” to the east, which is significantly deeper than the strait. The depth is relatively uniform on the eastern side of Björkö, but to the South the bathymetry shows a relatively gentle inclination upwards before it connects to the southern part of the shallow Björkö strait again.

Due to the focus of this thesis, the total study area is from now on referred to as “Area 1” and “Area 2”. Area 1 mainly corresponds to the Björkö strait, where the former harbor of Birka is included, while Area 2 is equal to the rest of the total study area (fig. 2.1).

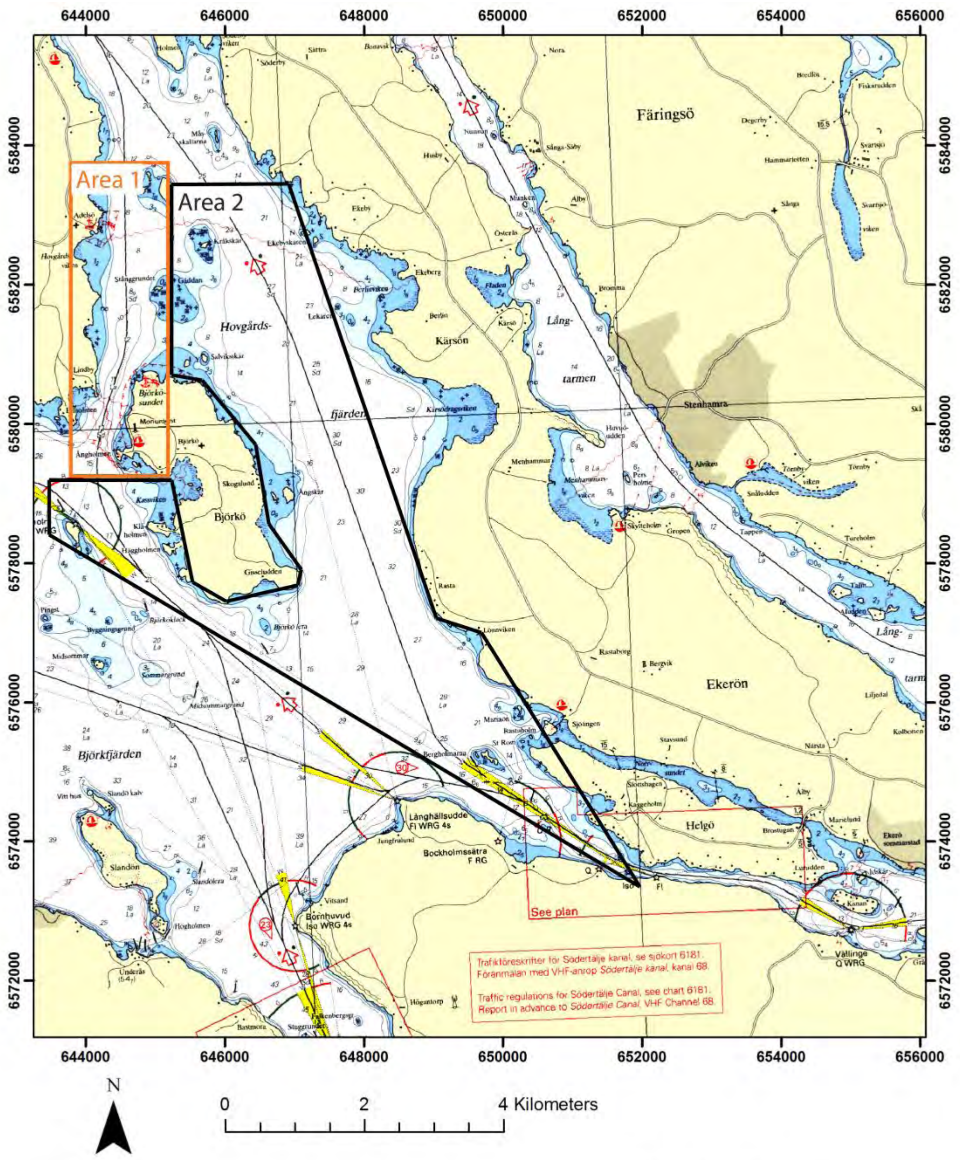

Figure 2.1. The study area is divided into ”Area 1” and ”Area 2”. Area 1 covers the Björkö strait where the potential to find archeological artifacts are highest. Therefore Area 1 will be the focus of this thesis. Basemap is from Sjöfartsverket navigational chart: Mälaren – Östra delen.

3. Material and Methods

3.1 Acoustic subbottom profiling

The basic idea of the penetrating echo sounder starts with a single frequency sound wave that is emitted towards the bottom. When the sound wave travels through one geologic material to another that differ in acoustic impedance, the sound wave acts as if it would be split into two parts. One portion will be reflected back where it will be registered by the acoustic receiver of the subbottom profiler, while the remaining part travels further down in the stratigraphic column until another acoustic impedance is encountered. Once again the sound wave splits in a reflected part that will be registered and a part that travels further down. This pattern repeats until the sound wave lost all its energy and becomes too weak to register. The acoustic impedance that causes the reflections of the acoustic pulses depends on the density of the material and the velocity of the sound wave passing through it. The higher the impedance contrast the clearer the acoustic reflection will be. Due to the density dependency of the acoustic impedance, it is often possible to distinguish and characterize different geological material from each other when studying the collected data. (Penrose et al., 2005).

The signal frequency of the subbottom profiler can be adjusted depending on the aim of the study. Lower frequency signals penetrates deeper into the sediment but on the expense of the resolution. Signals with higher frequency cannot reach as deep, but will instead give high resolute data from the relatively shallow stratigraphy (Penrose et al., 2005). The resolution of a specific subbottom data set can be estimated by simple calculations. There are two types of calculations which depend on which one of the two main types of subbottom profilers are being used (Jakobsson, 2012a). The first of the two types of subbottom profilers is the chirp. The chirp sweeps out sound waves in a preset bandwith defined by the minimum signal frequency subtracted from the maximum frequency of the signal. In this case, the resolution is roughly estimated by the following calculation:

$$R = V/(B * 2)$$

Where R is the resolution, V is the velocity of the sound wave and B is the bandwith of the sweeped out frequency.

The second type of subbottom profiler is the single beam penetrating echo sounder. Here the frequency is fixed and therefore the equation above is not valid. Instead the Rayleigh criterion is applied, which states that the thickness of an acoustic feature needs to be at least ¼ of the wavelength of the penetrating sound wave to be visible (Santamarina et al., 2005). Therefore, the resolution of the subbottom data in this case can be estimated according to the following formula:

$$R = (V/f)/4$$

Where R is the resolution and V and f are the velocity respectively the frequency of the sound wave.

For the subbottom profiling in this thesis, the single beam penetrating echo sounder Meridata MD500 was used. This echo sounder consists of a 28 kHz transducer mounted on a pole that was deployed over the side of the survey vessel. This gives relatively high resolute data from the uppermost 10 meters of soft sediments (Jakobsson, personal communication). To estimate the resolution in this case, the Rayleigh criterion should be used. This is done below with the sound speed assumed to be 1500 m/s which was used during the processing of the subbottom data in the Meridata suite:

$$\frac{\frac{1500\ m/s}{28000\ Hz}}{4} = 0.013\ m = 1.3\ cm$$

This means that in the case of the subbottom profiler data in this thesis, the vertical resolution is estimated to be 1.3 centimeters. However, in reality the broad opening angle of a single beam echosounder degrades the resolution substantially due to the wide horizontal foot print on the sea/lake floor.

3.2 Multibeam sonar

The original application of the multibeam sonar is to study bathymetry. This is simply derived from the two-way travel time for an emitted sound pulse that is traveling through the water column until it encounters the sea/lake bottom from where it is reflected back and registered. (Masetti and Calder, 2012).

In the case of a multibeam sonar, the basic theory above is applied on several sound pulses that simultaneously are being emitted from a transducer with a preset opening angle that decides the spread of the emitted sound pulses. The part of the seabed that is hit by the incoming sound pulses is called "swath with". To cover the sea/lake bottom of interest, the sound pulses will be emitted in a repeated pattern from the multibeam sonar during operation (Hamilton and Parnum, 2011). To be able to register the returning echo, it needs to be focused, or ensonified towards the survey. The whole swath width is not ensonified at once. Instead, the total swath width is divided into narrow strips or "footprints", where one footprint is ensonified at a time (Hell, 2011).

The area of a single footprint is dependent on the water depth from the transducer to the bottom together with the opening angle of the emitted sound pulses from the multibeam sonar. This relationship is also valid for single beam echosounders and can be explained by the following formula (Jakobsson, 2012b):

$$F = 2d \tan\left(\frac{a}{2}\right)$$

Where F is the footprint, d is the water depth from the transducer to the bottom and a is the opening angle of the sonar.

In addition to bathymetric data, multibeam sonars also collect backscatter data. Even though backscatter data was not the initial idea of the multibeam sonars, it has proven to be of greatest value for further information about the physical properties of the sea floor (Hamilton and Parnum, 2011; Le Bas and Huvenne, 2009).

Backscatter is a value of the retrieved energy of the reflected sound wave transmitted from multibeam echosounders and is measured in decibel (Masetti and Calder, 2012). The multibeam backscatter data is used for interpretation and characterization of the nature of lake and seabeds. Therefore, shallow water multibeam sonars operate in a relatively high frequency (100-800 kHz) which minimizes the penetration and gives high resolute data coverage of the bottom.

The backscatter data is based on the fact that a specific seabed type has a certain acoustic response controlled by the physical properties of the bottom. These properties mainly include grain size, roughness and density. Also the biology above the current area and the slope angle of the bathymetry can affect the acoustic response of the material (Hamilton and Parnum, 2011; Le Bas and Huvenne, 2009). In general, smoother and softer material (like clay, silt and loose sediments) produce a relatively weak returning backscatter signal, while rougher and harder material (like gravel, bedrock and compacted sediments) are indicated by significantly stronger signals (Rzhanov et al., 2011; Bellec et al., 2007).

During the backscatter data collection, several types of acoustic phenomenon may occur. Examples are the energy absorption of the water column and spreading of energy during the scattering of the sound pulses. These processes decrease the energy of the registered backscatter signals resulting in lower backscatter values. These noises may be compensated for during the post processing of the data (Masetti and Calder, 2012). The mentioned scattering of the sound pulses can also be an advantage which is presented below.

3.3 Angular range analysis

When the emitted sound pulses from the multibeam sonar hit the seabed, the energy will scatter. Here, one part of the scattered energy will find its way back along the angle of incidence, which eventually is the signal registered by the receiver of the multibeam sonar. The rest of the scattered energy will be redistributed in new directions, which therefore affects the backscatter result since it is not registered by the sonar. This factor is called “angular response factor”, and has a direct relationship with the angularity of the material on the seabed. If taken into account, the angular response factor can therefore hint about additional physical characteristics of the actual material on the seabed (Fonseca and Mayer, 2007; Fonseca et al., 2008).

“Angular range analysis” (ARA) is an analytical method that has been developed based on the angular response factor, which otherwise usually is lost during standard processing of backscatter data. The ARA method estimates the grain size, roughness and acoustic impedance of the sea floor by comparing the angular response data with an inverse mathematical model made for correlation between seafloor properties and acoustic backscatter observations. This method has proven to be a valuable tool for sea floor characterization due to its direct relationship with the material on the sea floor, which makes it less affected by noise than the regular backscatter signal (Fonseca et al., 2008).

The ARA method has been used in this thesis to estimate the sediment composition of the lake bottom in the survey area. A comparison with the acoustic subbottom profiles of the top layer of the stratigraphy has also been done, where differences and similarities are discussed.

The multibeam sonar used to collect the data analyzed in this thesis was a Kongsberg EM2040. This sonar can operate with frequencies in between 200 and 400 kHz (Kongsberg Maritime AS, 2012). During the majority of the data acquisition for this thesis, the multibeam operated with a frequency of 300 kHz which is optimal for shallow-water surveys (Kongsberg Maritime As, 2012).

To get multibeam sonar data of high accuracy, a motion sensor is needed that is capable of registering vessel motions that occur during acquisition (Kongsberg Maritime, 2010). During the survey in this case, a Kongsberg Seatex MRU 5+ was used which has a motion accuracy up to 0.01° for roll and pitch (Kongsberg Maritime, 2010).

Navigation during the data acquisition was acquired with a Hemisphere R320 GPS. RTK corrections were received from SWEPOS. RTK is an abbreviation for "real time kinematic", and gives a significantly refined position accuracy down to centimeter scale compared to the regular GPS (Reitdorf et al., 2006). To control the heading of the survey vessel, two "Hemisphere VS101" GPS compasses were mounted on each side of the Hemisphere R320 GPS.

3.4 Data processing and gridding

The data from the acoustic subbottom profiler were processed and interpreted using the Meridata software suite. Here Sview, a component of Meridata, was used for processing the raw data while MDPS was used for visualization of the data and interpretation of the acoustic units. These acoustic units were defined based on specific prominent reflectors. In most of the cases these reflectors were easily spotted. In some cases gas in the sediment disturbed the signal from the subbottom profiler. This made the interpretation of the acoustic units harder, sometimes even impossible.

The interpretations of the acoustic units in MDPS are along profiles, which mean gridding is necessary to make interpolated surfaces of these units. There are several types of gridding methods, and all of them have their own strengths and weaknesses. This means that the result will vary depending on the chosen gridding method. Therefore it is important to know the properties of a specific data set and what the aim with the surface modeling is (Burrough and McDonnell, 2009).

The interpreted data from MDPS were exported to the program Surfer (64 bit version 10.4) where the gridding method "Kriging" was used for each acoustic unit interpreted. Kriging is optimal for relatively sparse or irregularly spaced data sets (Burrough and McDonnell, 2009), which is the case in this thesis. To achieve an optimal grid for each acoustic unit, the settings sometimes differ regarding the grid size and search options for the different grids. Detailed grid reports for each gridded unit are presented in Appendix 8.1

The multibeam bathymetry raw data were treated in the Fledermaus suite, where Dmagic (64 bit version 7.3.2a) was used for gridding. Here the gridding type "Weighted moving average" was used to produce the interpolated surfaces of the survey area. This is the default gridding type in Dmagic which is suitable for large data sets. Area 1 was gridded with a cell size of 0.2 meters, while Area 2 was given a cell size of 0.4 meters. The reason for the difference in resolution is depending on two factors: 1. Area 1 is the area of focus where the chance to find archeological features are bigger than outside it, and 2. Area 1 has a higher density of data points which allowing a higher resolution.

After the data processing in Dmagic the gridded files were exported to Fledermaus (32 bit version 7.2.0). This was done to visualize and interpret the different features found in the data sets. Here it is also possible to clean data sets by deleting outlier data points that have resulted due to noise during the data acquisition. The cleanings are done by converting areas of interest to the file format "pure file magic" (PFM). By performing this file conversion outlier soundings can relatively easily be deleted from the data set (Mallace and Gee, 2005). This process was done for the confirmed ship wreck "Marjaana" gridded in the cell size of 0.2 meters. To get an idea about the shape of the ship a painting of Marjaana was used as a template during the editing of the 3D model. In addition to Marjaana, two other 3D models of shipwrecks are presented in this thesis. The PFM files corresponding to these models were gridded in the cell size of 1.0 meters due to sparser data coverage compared to Marjaana.

The multibeam backscatter data was processed in FM Geocoder (7.3.1a 64 bit) which also is a part of the Fledermaus suite. Here backscatter mosaics and angular range analysis (ARA) were produced for both Area 1 and 2. The mosaic resolution for Area 2 was made in 0.3 meters while the corresponding resolution for Area 1 was made in 0.04 meters. The reason for the significant difference in mosaic pixel size is the same here as in the case of the multibeam bathymetry data, but is in this case of greater importance due to the ability of the backscatter data to locate and interpret features on the lake floor with a higher resolution than the bathymetry data.

Important to note is that the given cell sizes for both the multibeam bathymetry and the backscatter data will affect the details and dimensions of objects spotted in the data sets. Therefore it is of greatest significance to grid the actual data set in such a small cell size as possible which in turn increases the detail visibility of the data.

After the data processing in FM Geocoder, the mosaic and ARA files were just like the gridded files from Dmagic exported to Fledermaus (32 bit version 7.2.0) for visualization and further interpretation.

The bathymetric and backscatter maps were in the end combined with navigational charts using ArcMap (10.1) to get a better understanding for the orientation of the localized features in the data sets.

It should be noted that the multibeam bathymetry data set used in this thesis also has been processed in the Caris suite where the RTK correction is used to correct for ship heave and water level fluctuations during the survey period. This work was done by Martin Jakobsson, who is professor in marine geology and geophysics and supervisor of this thesis.

4. Results

4.1 Acoustic subbottom profiling

In total, five acoustic units (U1-U5) were defined in the survey area. U1 is found deepest in the profiles (oldest) and U5 is situated in the top (youngest). The acoustic characteristics of these units are presented in table 4.1.1.

Before the description it should be stated that the black soil situated in the former harbor area of Birka (fig. 1.1) could not be identified in the subbottom data. This may depend on several factors like the sonar and its resolution, the data processing or the nature of the sediment layer and its location on shallow bedrock.

Acoustic unit	Acoustic characteristics	Representative example
U5	Acoustically, U5 is semitransparent and has no sign of internal reflectors. The maximum thickness recorded for U5 is 0.5 m. This is the youngest of all the acoustic units.	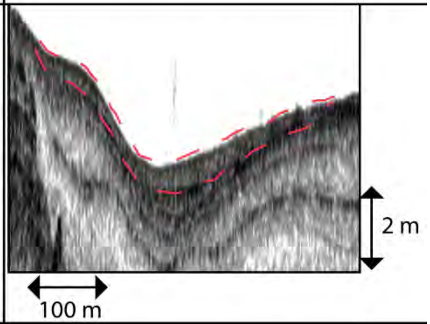
U4	This opaque surficial unit is the dominating top unit. The maximum thickness recorded for U4 is 0.5 m.	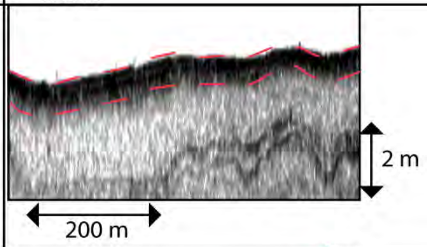
U3	This unit is acoustically transparent to semitransparent. Weak, internal reflectors do exsit but are rare. The maximum thickness recorded for U3 is 3.0 m. This unit also ends with a sharp reflector to the next unit.	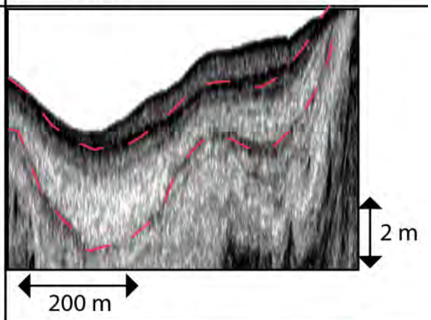
U2	U2 is acoustically semitransparent with relatively diffuse internal reflectors following the same pattern as the ones inside U1. The maximum thickness recorded for this unit is 5.0 m. U2 also ends with a sharp reflector to the next unit.	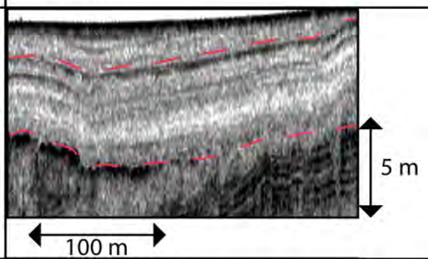
U1	This unit contains several internal sharp reflectors that lie parallel to each other and to the underlying bedrock. The maximum thickness recorded of U1 is 10.5 m and ends with a sharp reflector to the next unit.	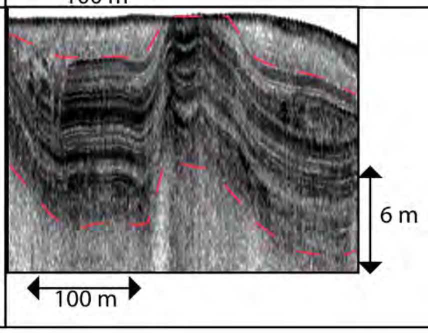

Table 4.1.1. Five acoustic units (U1-U5) were defined in the study area. U1 is found deepest (oldest) and U5 is located in the top (youngest). The acoustic characteristics for each unit are found here together with the respective unit highlighted with red stripes.

The acoustic units from table 4.1.1 are here presented in relation to each other by using parts of four profiles (figs. 4.1.2-4.1.5) showing the stratigraphy of the acoustic units. To get an idea of the location of these profiles, the corresponding survey lines and the respective profile number are shown on the map in figure 4.1.1.

The two first profiles SBP 15161846 and SBP 15181403 (figs. 4.1.2 and 4.1.3) are both from Area 1 (fig. 4.2.1). Both these profiles are of relatively high quality even though gas is apparent in figure 4.1.2 which disturbs U1. In both profiles it is possible to see that U1 and U2 are the dominating units regarding both thickness and distribution. U1 is found virtually everywhere, while U2 lacks in a few spots (fig. 4.1.2). U3 on the other hand, is significantly thinner than the two previous units but also shows a less areal distribution. The latter difference is clearer in Area 2 and will therefore be presented later.

The figures 4.1.2 and 4.1.3 also show that the relatively thin U4 is virtually found everywhere. This is the dominating surfical unit except when it is followed by U5. U5 is the youngest and least distributed acoustic unit in the whole study area. This unit is found in four individual locations in Area 1, where one of the locations covers a significantly bigger area and volume compared to the other three (fig. 4.1.2).

Area 2 (fig. 4.1.1) is here represented by the acoustic profiles SBP 15161404 and SBP 15161129 (figs. 4.1.4 and 4.1.5). These profiles also show that U1, U2 and U4 are virtually found everywhere while U3 is less distributed. U3 tends to be located in bathymetrical sinks, and is therefore less distributed than the corresponding unit in Area 1. It is also evident that U5 is absent in Area 2 (figs. 4.1.4 and 4.1.5).

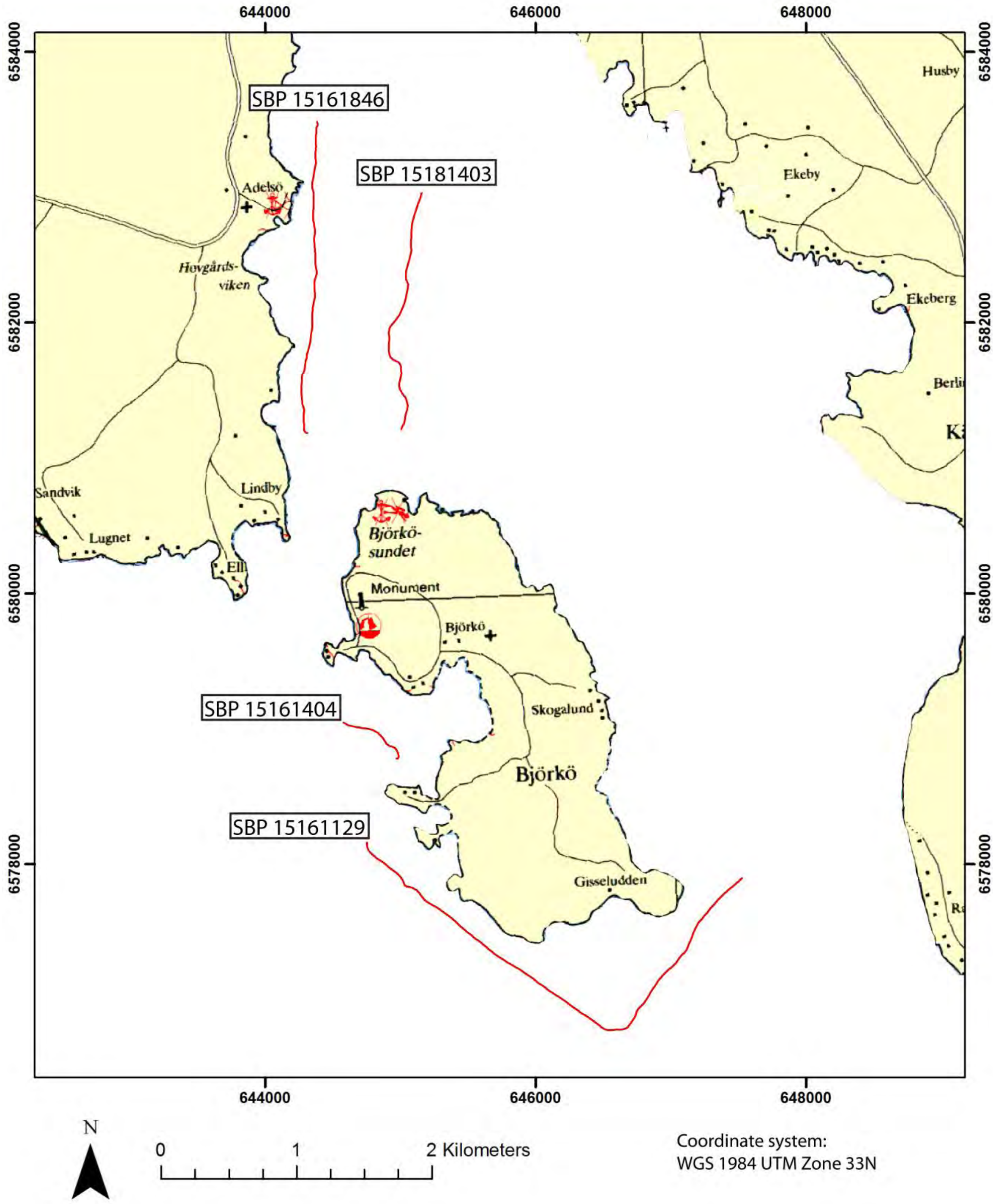

Figure 4.1.1. Location of the four survey lines (red) corresponding to the subbottom profiles presented in the text and the figures 4.1.2-4.1.5. The two northernmost survey lines (SBP 15161846 and SBP 15181403) represent Area 1 while the other two (SBP 15161404 and SBP 15161129) are from Area 2. Basemap is from Sjöfartsverket navigational chart: Mälaren – Östra delen.

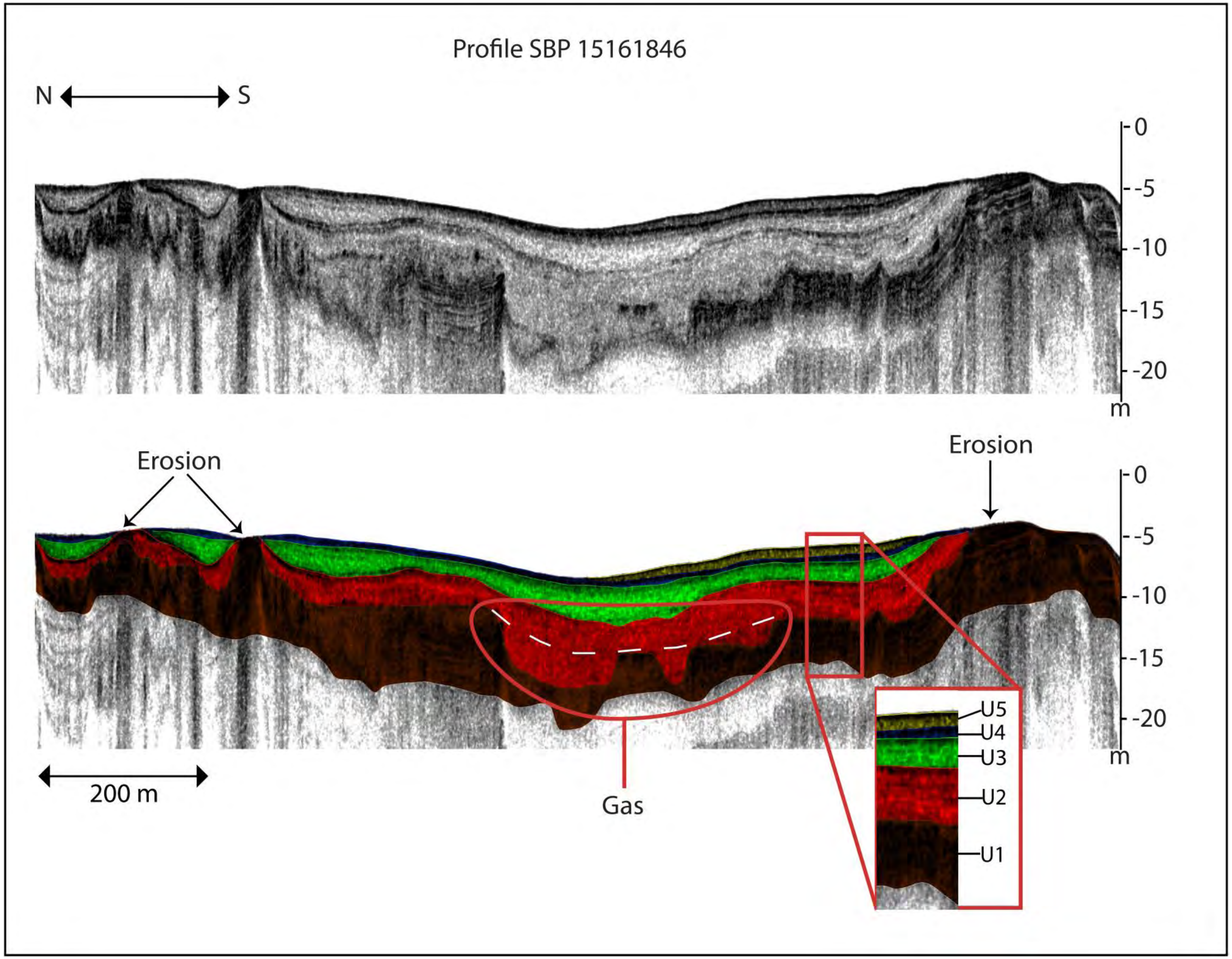

Figure 4.1.2. Uninterpreted (top) and corresponding interpreted (bottom) part of the acoustic profile SBP 15161846 from Area 1. Here all the five acoustic units are represented, where U1 and U2 are the most dominant ones. Erosion and gas emit are affecting the profile, where the latter process disturbs the acoustic signal as seen in the red ellipse. Inside the red ellipse there is a striped white line which indicates the probable extension of U1 in this case.

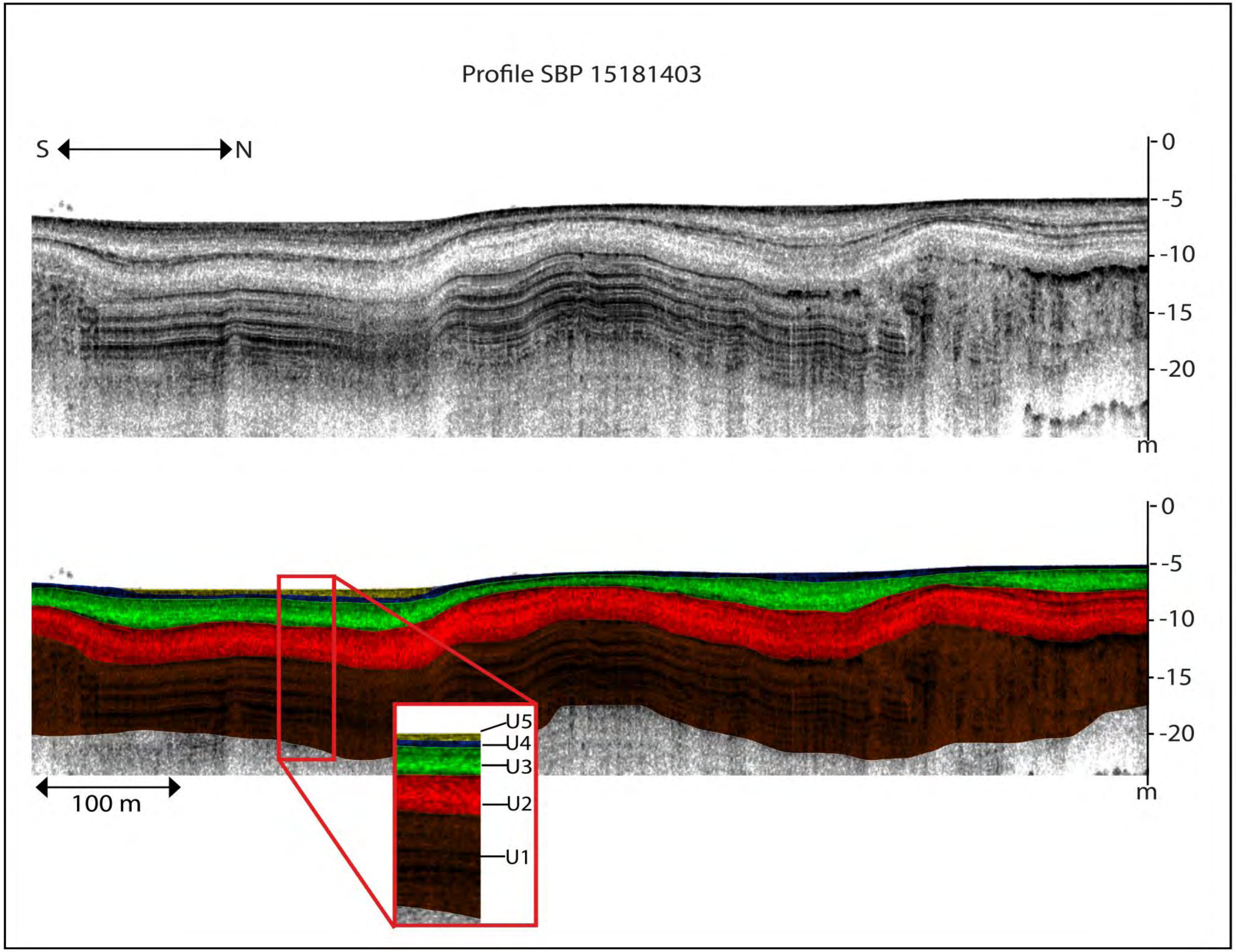

Figure 4.1.3. Uninterpreted (top) and corresponding interpreted (bottom) part of the acoustic profile SBP 15181403 from Area 1. Here all the five acoustic units are represented, where U1 and U2 are the most dominant ones.

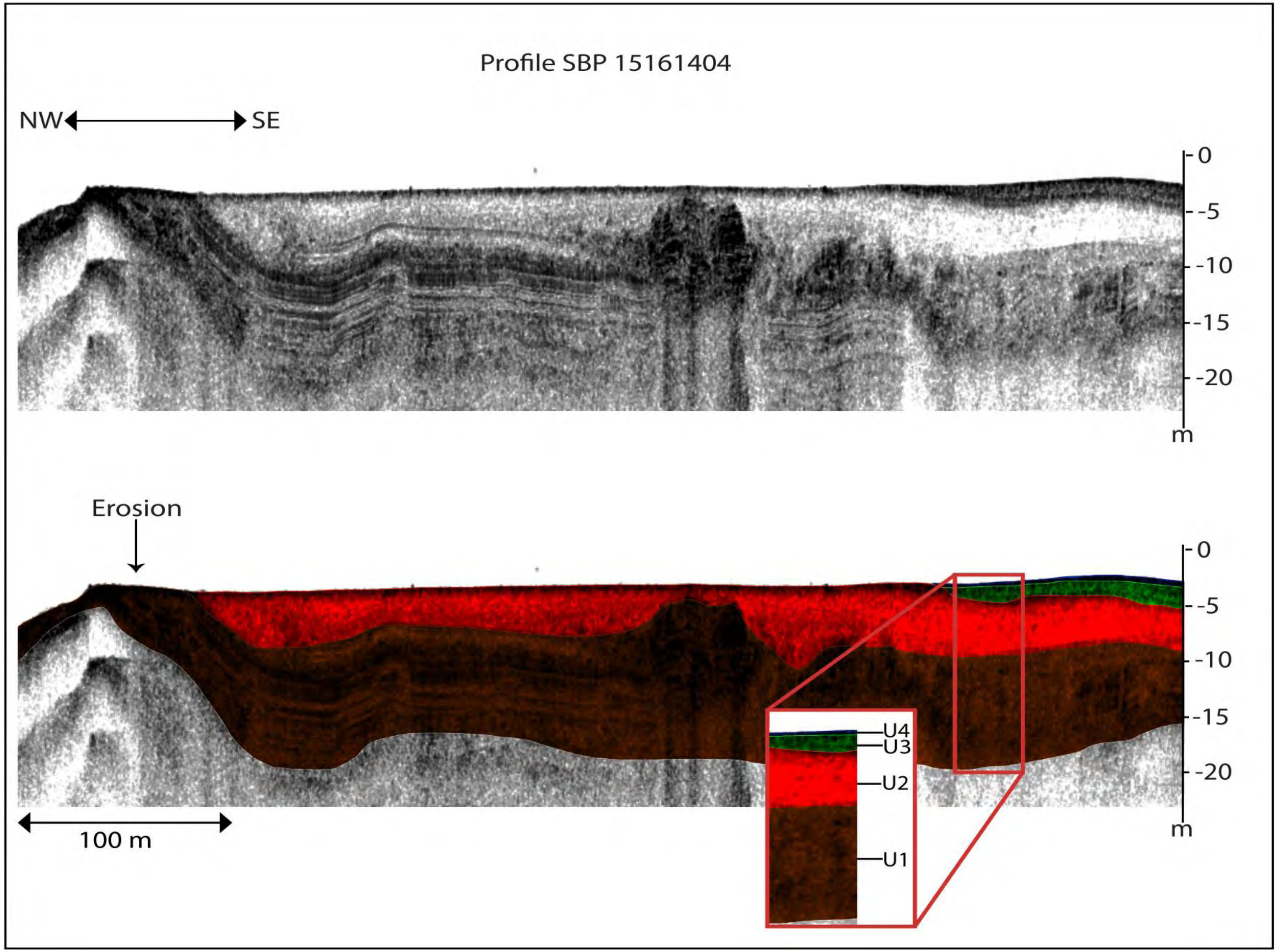

Figure 4.1.4. Uninterpreted (top) and corresponding interpreted (bottom) part of the acoustic profile SBP 15161404 from Area 2. Here U1 to U4 are represented, where U1 and U2 are the most dominant ones while U3 is less distributed than in Area 1. U5 does not exist in Area 2.

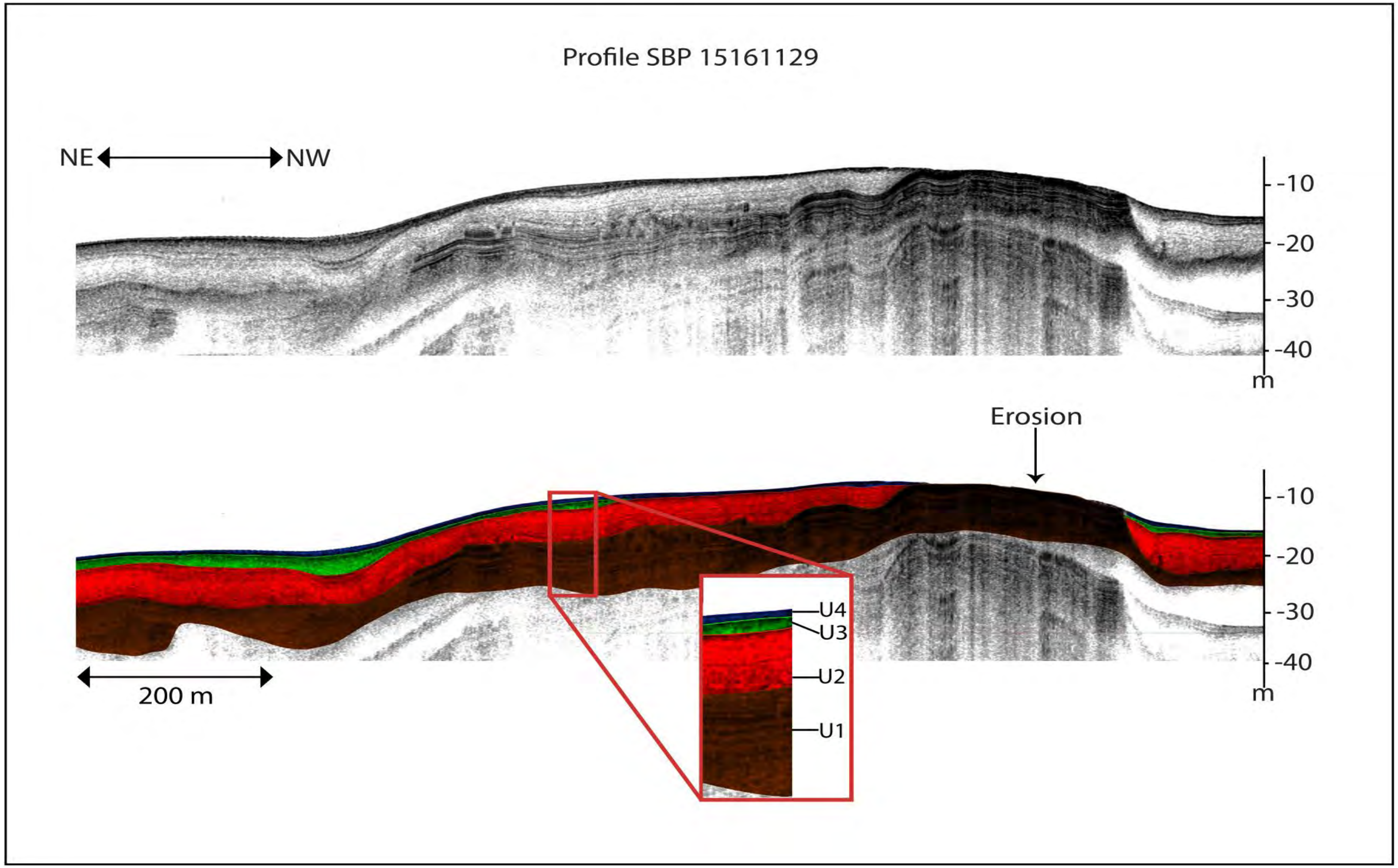

Figure 4.1.5. Uninterpreted (top) and corresponding interpreted (bottom) part of the acoustic profile SBP 15161129 from Area 2. Here U1 to U4 are represented, where U1 and U2 are the most dominant ones while U3 is less distributed than in Area 1. U3 has a tendency to be situated in bathymetrical sinks in Area 2, which is the case in this figure. The profiles of Area 2 are commonly affected by more erosion than the ones of Area 1. U5 does not exist in Area 2.

Figure 4.1.6 shows a distributional pattern for the acoustic units (except U4) exposed at the lake floor in Area 1. U4 has been left out since it corresponds to a relatively thin surficial unit that is virtually found everywhere. Without this unit the erosional patterns are easier to detect, which also could be of significant value for locating archeological artifacts.

In figure 4.1.6 below, it is possible to see that erosion is more common in the southern part of Area 1 than in the middle and northern parts. The erosion mainly reaches down to U2, which in these areas often is the unit exposed at the lake floor. Also note the four individual spots (yellow) that correspond to the total areal distribution of U5. U5 is totally absent in Area 2 (fig. 4.1.7). Further, figure 4.1.7 indicates erosion mainly along the eastern coast of Björkö, where U1 is exposed at the lake floor. This is true also for a relatively small area in the West. Erosion is also present to the North, but there reaches mainly to U2 (fig. 4.1.7).

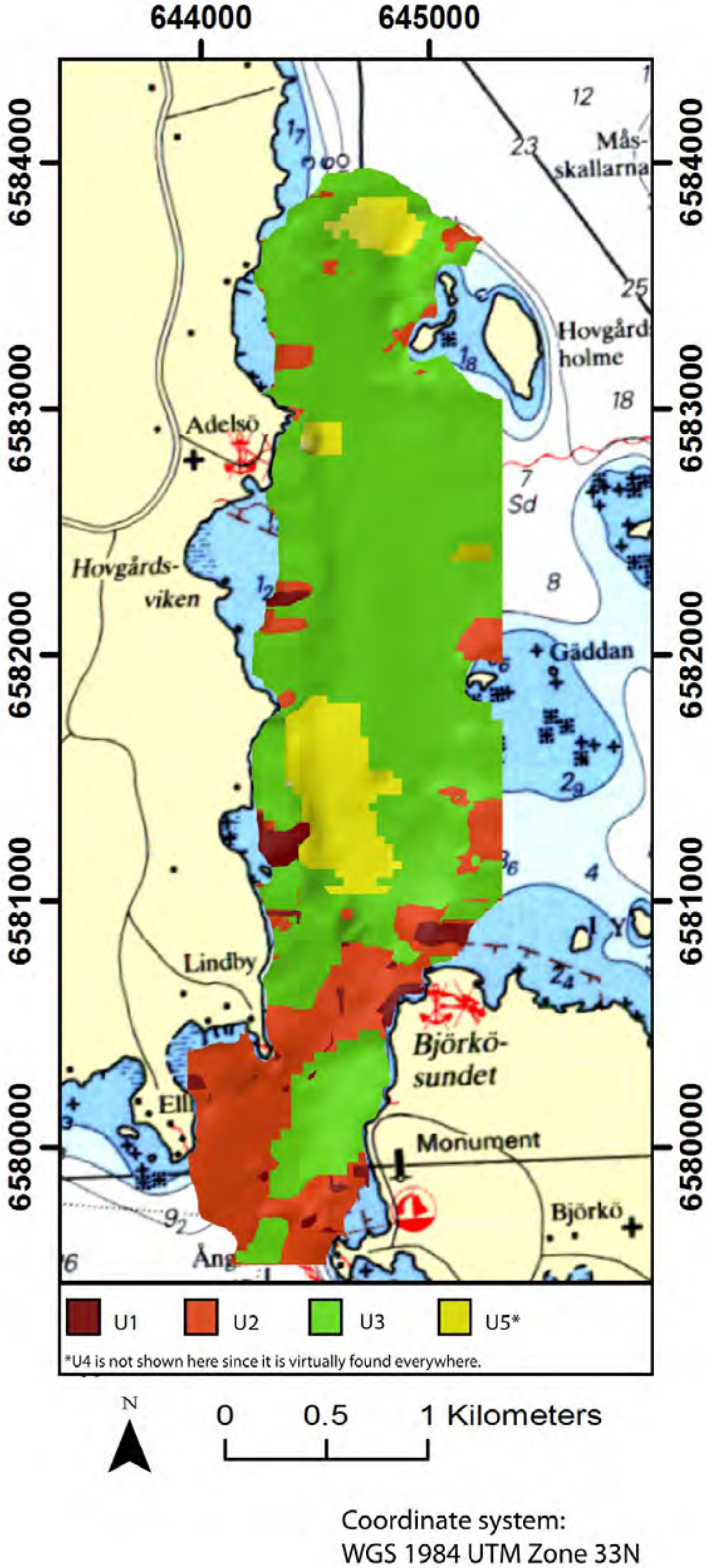

Figure 4.1.6. The areal distribution of the acoustic units on the bottom surface of Area 1, where U1 is the bottom unit and U5 is in the top. U1 covers the whole Area 1, while U2 lacks in a few spots. U3 is most dominant in the upper to the middle parts of the area, while U5 is the unit of least extension, mostly found in the middle of Area 1. Basemap is from Sjöfartsverket navigational chart: Mälaren – Östra delen.

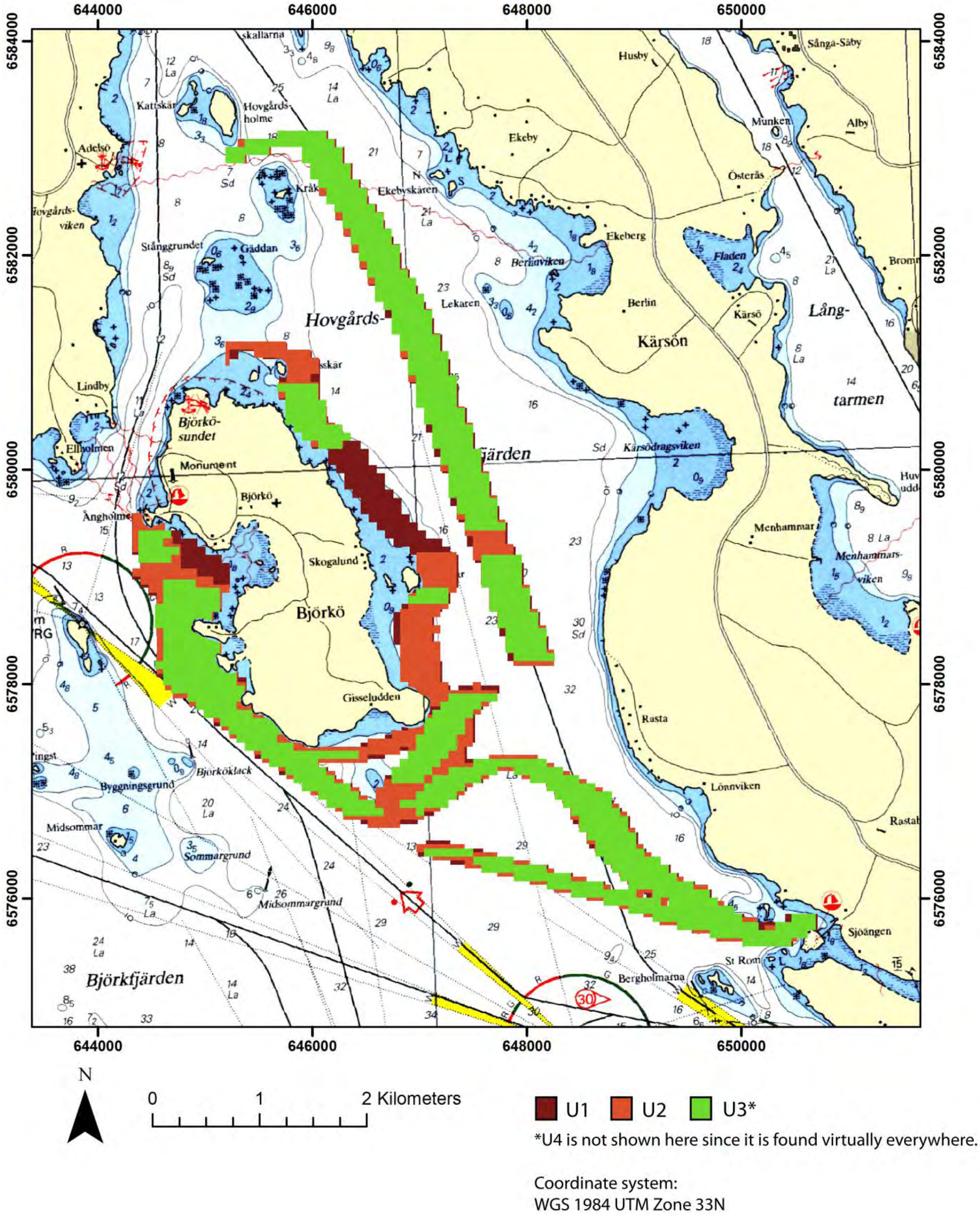

Figure 4.1.7. The areal distribution of the acoustic units on the bottom surface of Area 2, where U1 is the bottom unit and U3 is in the top. U1 covers the whole Area 1, while U2 lacks in a few areas. The absence of U3 is most dominant to the East coast of Björkö. Basemap is from Sjöfartsverket navigational chart: Mälaren – Östra delen.

4.2 Point objects

23 individual objects standing upright from the lake bottom were spotted in the acoustic subbottom profiles from different locations around the island of Björkö. Since the origin of these objects have not been verified, they will from now on be called “point objects”. Depending on the acoustic characteristics of the point objects, they have been sorted into three different types (table 4.2.1). Before presenting the three types it should be stated that it is not clear how much the point objects differ from each other in reality.

Point type	Acoustic characteristics	Representative example
Type 1	13 of all the 23 point objects have been characterized as Type 1 point objects, and are therefore the most common type. Acoustically, the point objects of this type are relatively diffuse - weak contours with sharpened tops are vissible standing on a depth of 6 to 7 m. The average height of this point type is 3.2 m, while the width varies from 3 to 6 m.	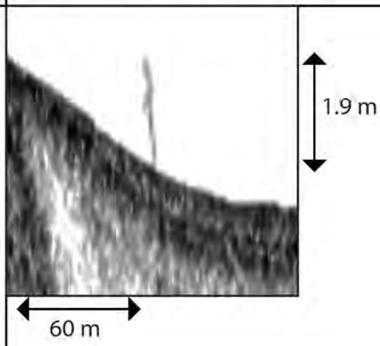
Type 2	Eight of all the point objects have been characterized as Type 2 point objects. The average height of the point objects in this group is 0.8 m. This makes this type significantly smaller than Type 1. The width cannot be measured accurately since it is too narrow for the subbottom data to register. Excpt the size difference, Type 2 is acoustically clearer and therefore easier to spot.	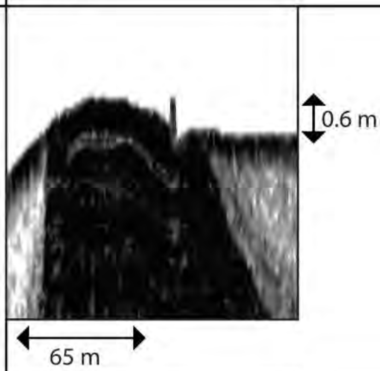
Type 3	Two of all the point objects have been characterized Type 3 point objects. The average height of the objects in this group is 2.3 m and the width is 5 m. Acoustically this type reminds of Type 1, but is just like Type 2 clearer and therefore fully visible in the water column.	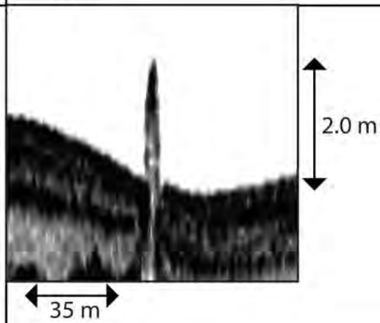

Table 4.2.1. In total 23 point objects were found in the survey area. They have been divided into three different types depending on their acoustic characteristics. These three types are presented in this table.

The three types of point objects are plotted in figure 4.2.1 together with an already confirmed water palisade after Ingelman-Sundberg (1972). Here it can be seen that the Type 1 point object mostly is found within a certain area in the Björkö strait (fig. 4.2.1, box A). In this area, four of the Type 1 point objects are on a straight line situated with relatively even spacing (150 to 200 m). The same area coincides with the location of the thickest and the most-wide spread of the four U5 units.

When it comes to the geographical distribution of the Type 2 point objects, figure 4.2.1 shows that this type is found sparsely along the coastline of Björkö situated on bathymetrical heights on an approximate depth of 4 meters.

The two objects that together form the Type 3 point objects are found relatively close to each other outside the western coast of Björkö on an approximate depth of 5 meters (fig. 4.2.1).

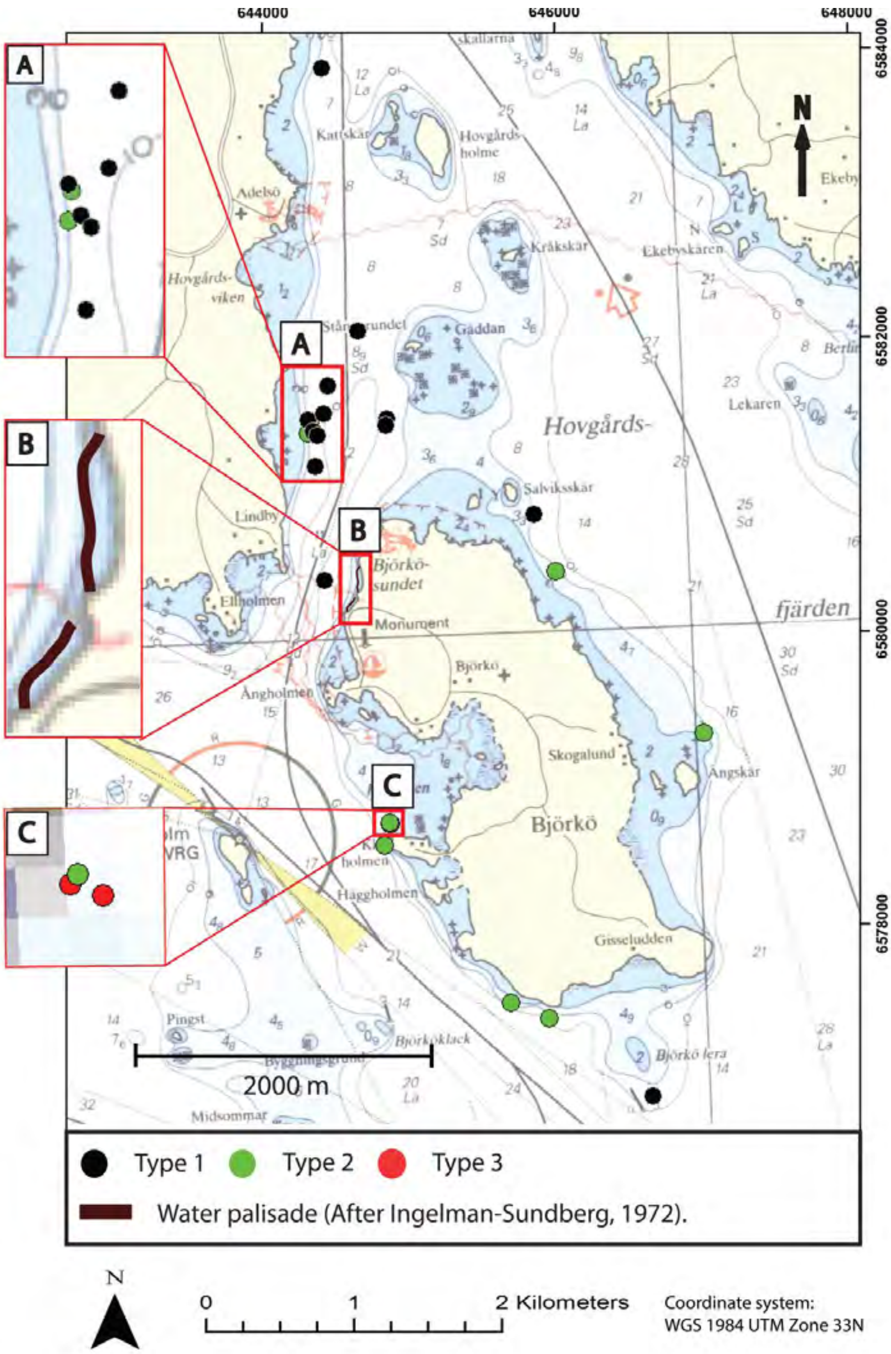

Figure 4.2.1. Geographic distribution of the three types of point objects categorized according to their acoustic properties in the subbottom profiler data. Here they are presented in relation to the confirmed water palisade after Ingelman-Sundberg, (1972). Note the area in box A where the point objects are situated relatively dense within the U5 sediment unit. Four of these point objects also show a relatively regular spacing in between each other. Basemap is from Sjöfartsverket navigational chart: Mälaren – Östra delen.

4.3 Multibeam bathymetry

Figure 4.3.1 shows the multibeam bathymetry from the complete survey area of this study. Over all, this is a relatively shallow area where the depth range varies from 2 to 32 m. The deepest parts are found in the south-eastern part of the area while the shallowest parts are found in Area 1 (lighter colors in fig. 4.3.1), which also was described in Study area.

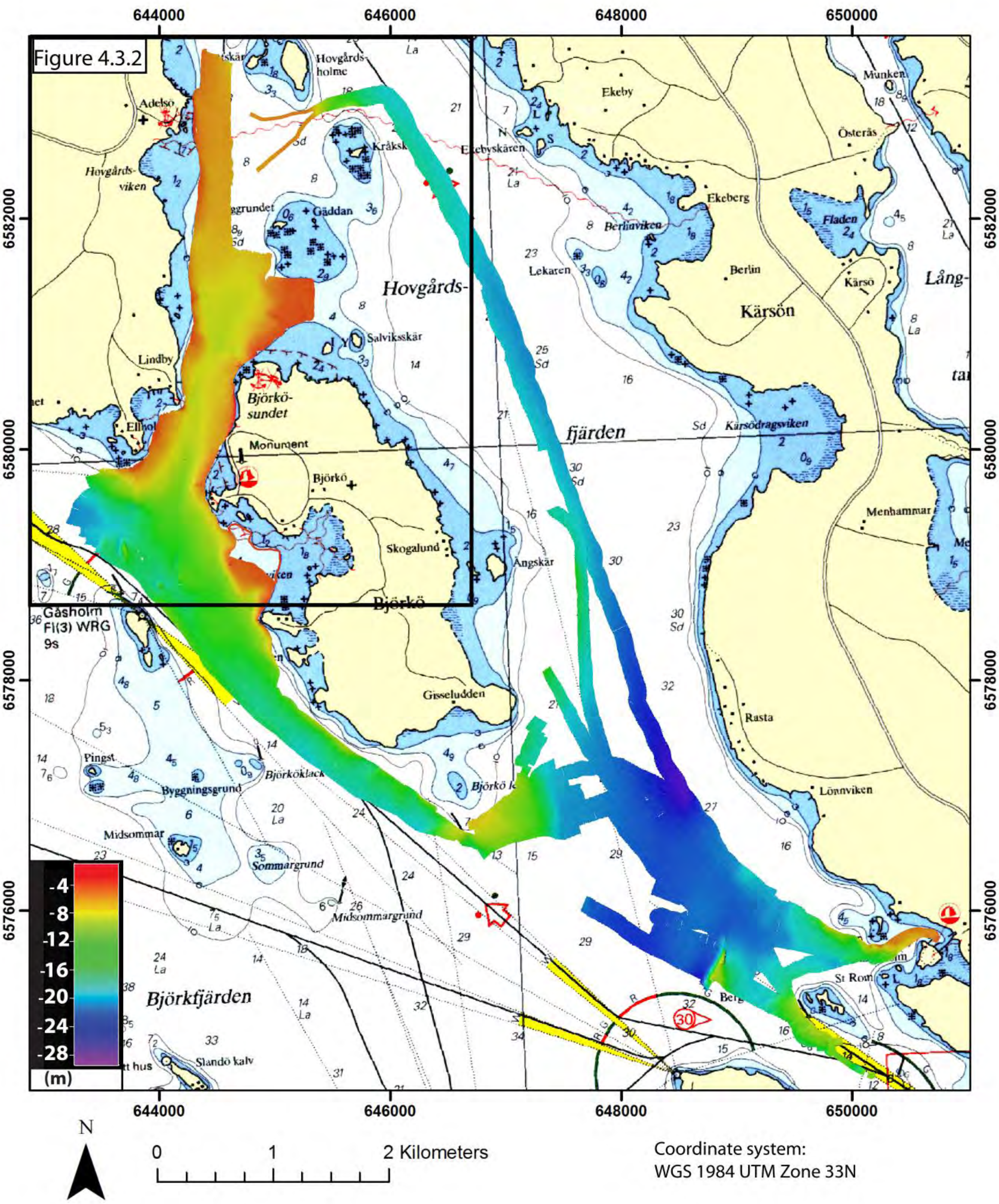

Figure 4.3.1. The gridded multibeam echo sounder bathymetry data for the total survey area, where darker colors indicate deeper areas. Area 1 is marked by the black box (fig.4.3.2). Basemap is from Sjöfartsverket navigational chart: Mälaren – Östra delen.

In the multibeam echosounder data covering Area 1, several features of interest were characterized based on their visual appearance in the data set. These features will from now on be referred to as "ES features". Most of the ES features are subdivided into several objects that have a similar appearance in the data set. These objects are from now on referred to as "ES objects". From now on, a series of ES features that represent the data covering Area 1 will be presented. The respective location for each ES feature is highlighted by red circles/ellipses in figure 4.3.2.

Before the presentation of the ES features it should be stated that the harbor area of Birka (fig. 4.3.2) naturally is an interesting place for archeological artifacts. Several objects of interest have been spotted here. Due to the small dimensions and low relief together with significant differences in acoustic response of these objects compared to the lake bottom, they are better viewed in the backscatter data. Therefore, the harbor area will in the case of the multibeam echosounder data not be considered.

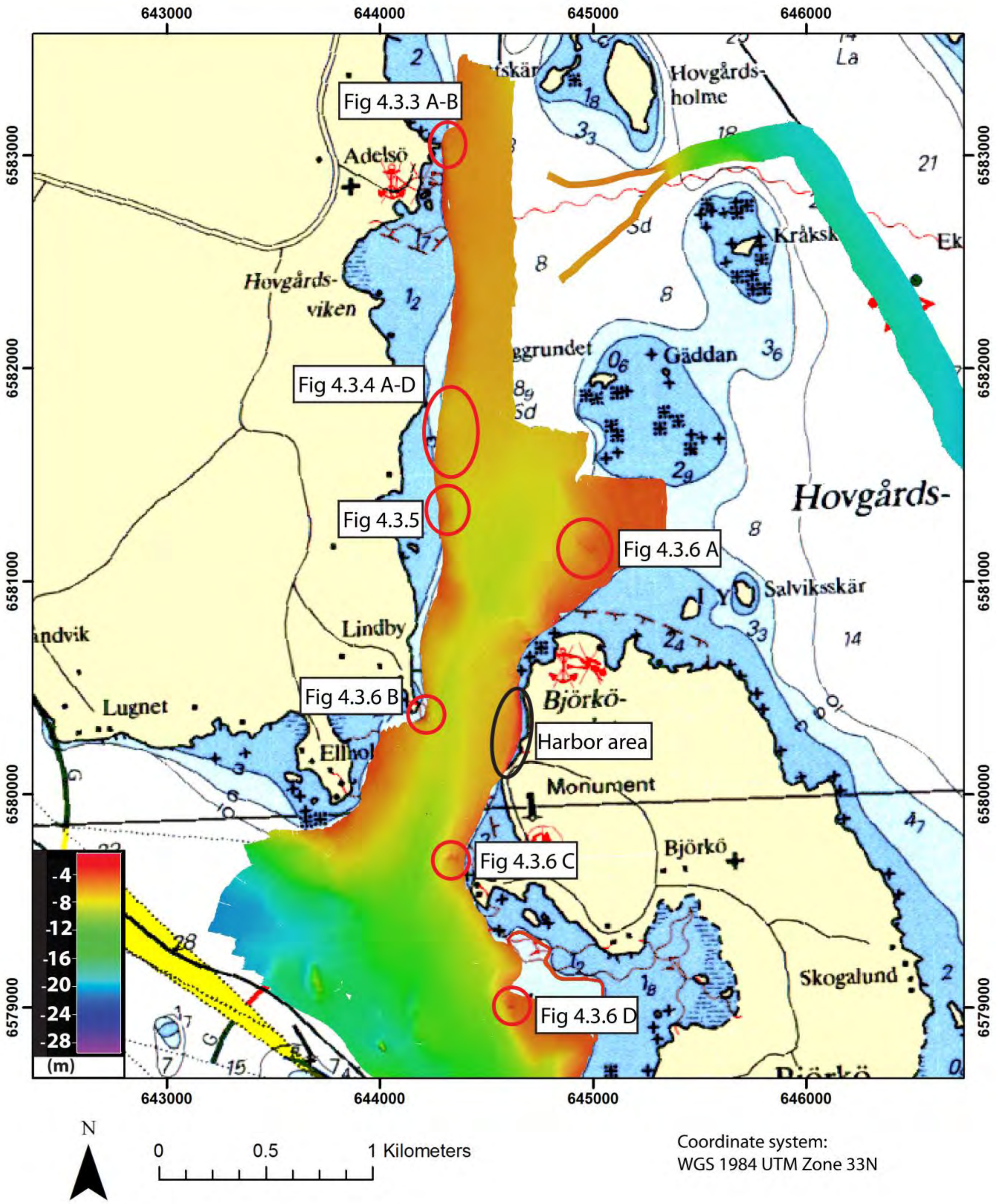

Figure 4.3.2. The gridded multibeam echo sounder bathymetry data for Area 1 where darker colors indicate deeper areas. The numbered circles/ellipses are highlighting the locations for specific ES features that are presented in the text below. The black ellipse is in this case highlighting the harbor area of Birka. This area will not be considered here but will instead be treated in the backscatter result. Basemap is from Sjöfartsverket navigational chart: Mälaren – Östra delen.

ES feature 1

This ES feature is found in the northern part of Area 1 (fig. 4.3.2) and consists of a fan shaped pile of loose material originating from the steeper part of the bathymetry (fig. 4.3.3A). The maximum width and height of the fan is 35 respectively 0.6 m (fig. 4.3.3B).

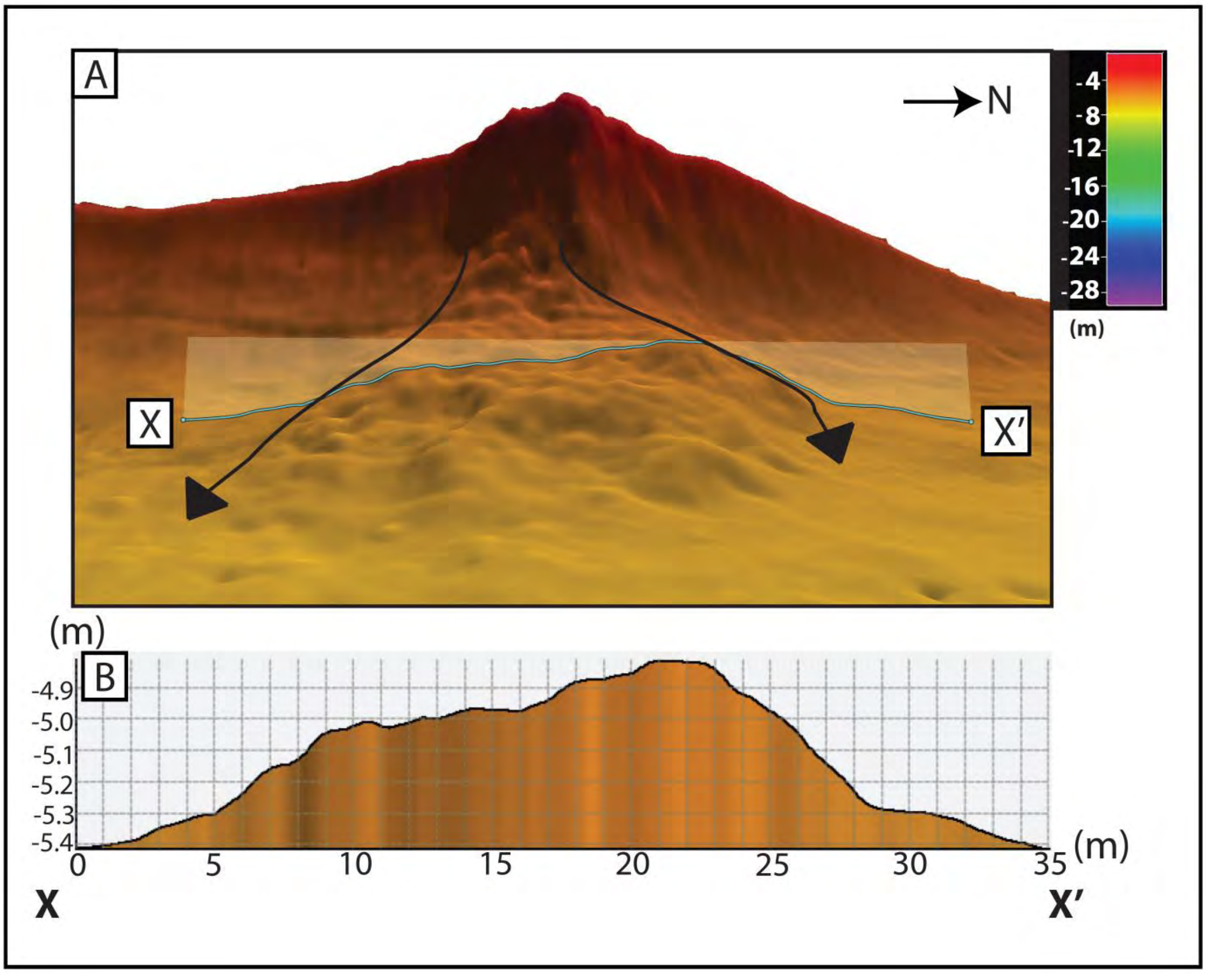

Figure 4.3.3. ES feature 1. Fan shaped pile of relatively loose material originating from the steeper part of the bathymetry indicated by black arrows (A) and a cross cutting profile of it (B).

ES feature 2

Here four ES objects have been grouped together because they are all located relatively close to each other on the Adelsö side of the strait on a depth of approximately 8 meters (fig. 4.3.2). They also have relatively similar dimensions, where the length of the objects varies in between 6 and 14 m while the height above the lake bottom never exceeds 15 cm (fig. 4.3.4 A-D).

It should be mentioned that the diffuse stripes that are visible in all the cases in figure 4.3.4 are offsets in between swaths. These offsets usually have heights varying in between 20 and 25 cm. A clear example is highlighted by a red ellipse in figure 4.3.4D.

When it comes to the origin of the objects in figure 4.3.4 there is a possibility that object B is a print in the bathymetry after a data collection by Sjöfartsverkets (Swedish Maritime Administration) (Jakobsson, personal communication). The origin of the other three ES objects (A, C and D) are unknown.

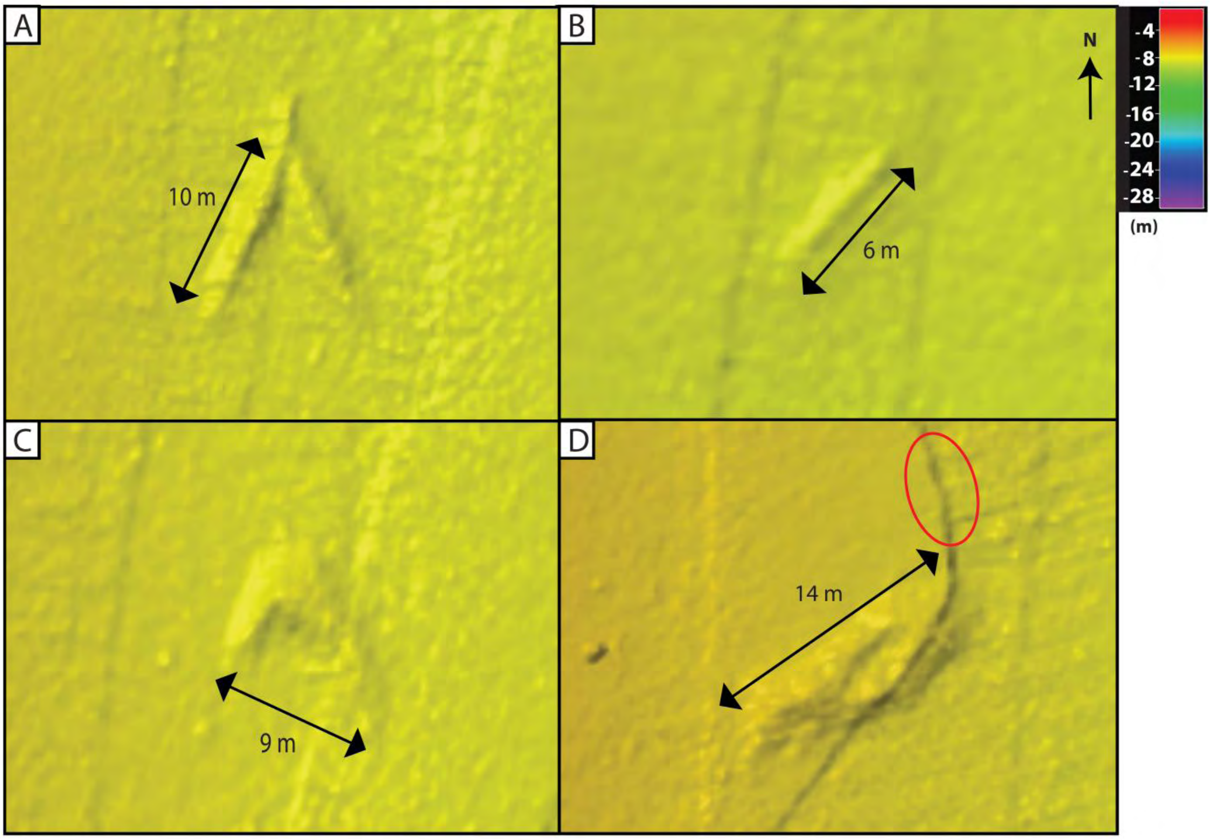

Figure 4.3.4. ES feature 2 consists of a group of four objects in the bathymetry on the Adelsö side of the Björköstrait. While B probably is a print in the sediment from a previous data collection, A, C and D are of unknown origin. The diffuse lines seen in each figure are caused by offsets in between swaths. The red ellipse in D highlights a relatively easily detected example of these noises.

ES feature 3

Figure 4.3.5 is a representative example of the bathymetry from an area corresponding to a single "Type 1 point object" located in the area of the biggest patch of the U5 acoustic sediment unit (fig. 4.2.1 box A). This rough patch in the otherwise relatively flat bathymetry covers an area of 5×4 m, where the tallest peaks reaches about 20 cm up into the water column (fig. 4.3.5). The majority of the locations represented by "Type 1 point objects" are covered by similar features as the one in this case. In the few cases where this connection cannot be made, the bathymetry is flat. This means that the clearly visible Type 1 point objects from the subbottom profiler data are not present in the multibeam bathymetry data. What causes this significant difference in the two different data sets will be treated in the discussion.

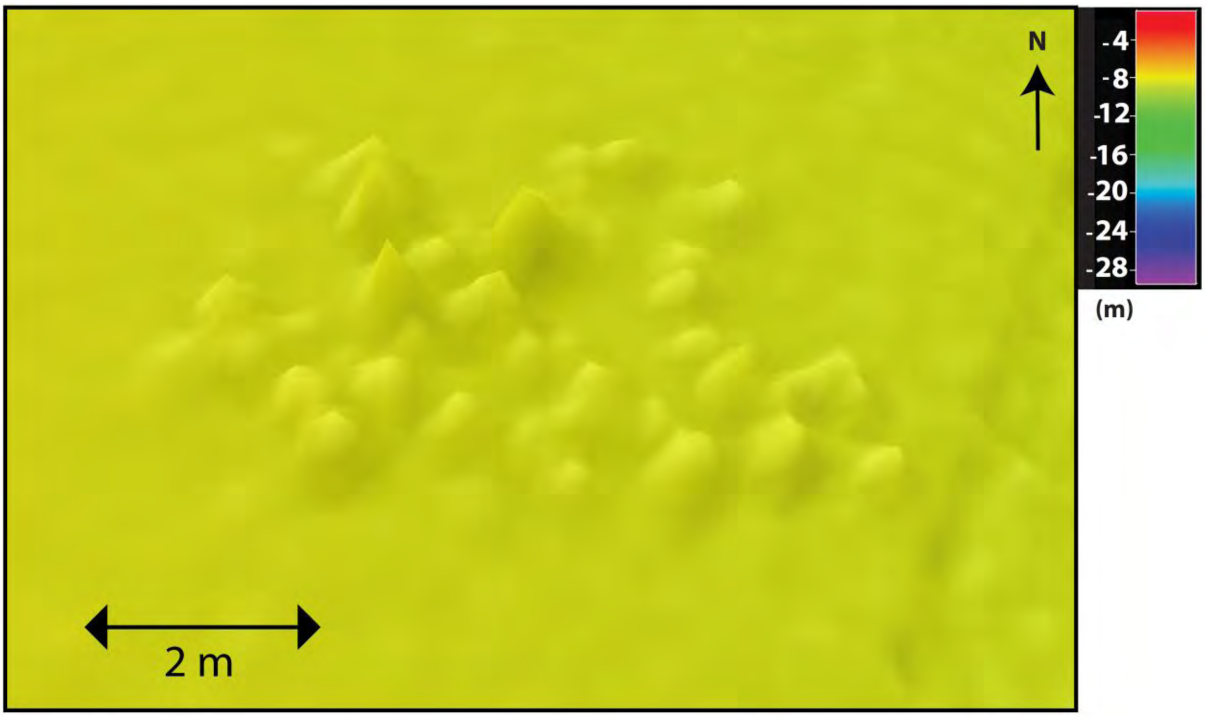

Figure 4.3.5. ES feature 3. A representative example of the bathymetry from an area corresponding to a single Type 1 point object. This indicates that the Type 1 point objects spotted in the subbottom profiler data shares no visual similarities with the corresponding areas in the multibeam bathymetry data. This connection is true for most of the locations that corresponds to a single Type 1 point object. In the few cases where this connection cannot be made, the bathymetry is flat.

ES feature 4

In this case four ES objects have been grouped together due to their similarities in visual appearance (fig. 4.3.6A-D). These objects can all be described as pointy objects on top of relatively elevated parts of the lake bottom. Several other objects that fit into this description have been localized within Area 1. The four examples in this case (fig. 4.3.6A-D) are the most prominent and representative examples.

The geographical distribution shows that A, C and D (fig. 4.3.6) are all found offshore Björkö on a depth from 5 to 8 m (fig. 4.3.2). Of these three ES objects, dimensional similarities exist in between the pointy objects on top where the heights vary in between 0.3 and 0.9 m while the widths tend to be from 0.5 to 2 m. The distributions of these pointy objects tend to be random in all cases except in the case of object D where six of the latter objects are situated in a bow-shaped formation facing the deeper parts of the bathymetry. The distance in between these pointy objects varies from 9 to 16 m (fig. 4.3.6D).

Object B in figure 4.3.6 is the only one of the four objects in figure 4.3.6A-D that is present on the Adelsö side of the strait (fig. 4.3.2). It is also directly connected to the shore unlike the other three. The pointy objects within object B are denser situated but also smaller (maximum height is 0.5 m and the maximum width is 2 m).

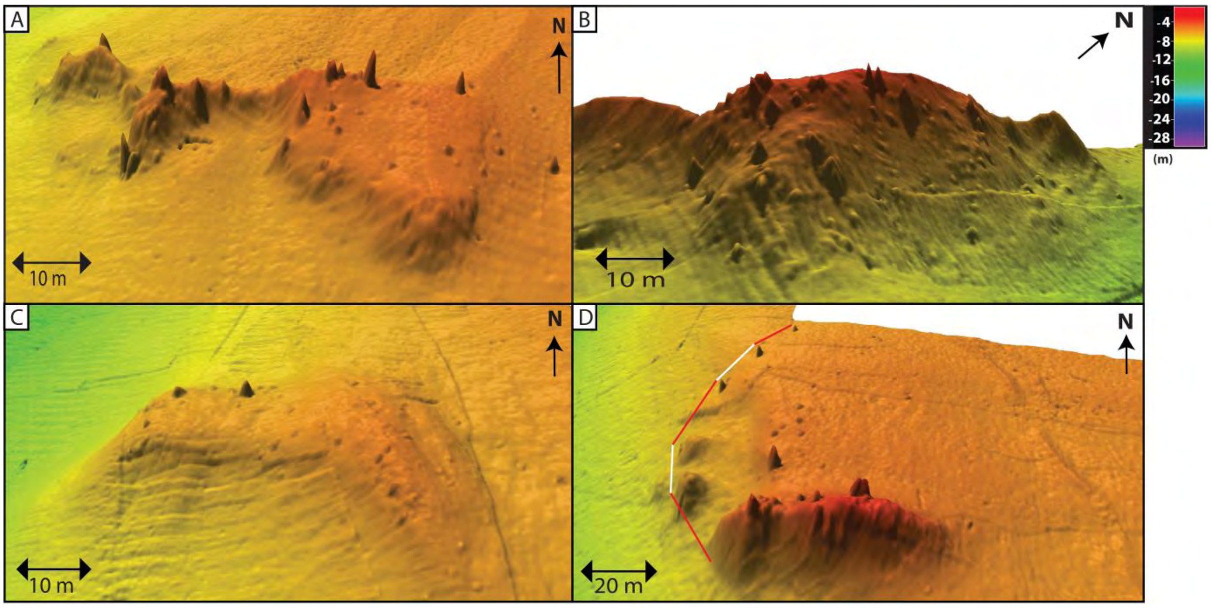

Figure 4.3.6. ES feature 4 consists of four examples where the bathymetry is relatively elevated and contains pointy objects on top that usually are randomly distributed except in case D where the white and red line highlights a possible pattern that the pointy objects follow.

4.4 Multibeam backscatter

Figure 4.4.1 shows the multibeam backscatter result for the entire survey area. The backscatter values display relatively small variations, generally in between -30 and -40 dB. Higher backscatter values are, however, found in Area 1 where they often reach -20 dB (fig. 4.4.2). The backscatter features of interest henceforth referred to as BS features will from now on be presented. Focus will just like in the case of the ES features be put on the BS features of Area 1. These BS features are all highlighted in figure 4.4.2. Most of these BS features correspond to the ES features described before. The only difference is the BS features from the harbor area of Birka, which exclusively are presented here.

After the presentation of the BS features of Area 1, focus will be put on Area 2. The focus of the BS features of the latter area will exclusively be put on shipwrecks. The respective location of these shipwrecks is presented as red and black circles in figure 4.4.1. The red circles correspond to already registered shipwrecks, while the black circles indicate unregistered wrecks.

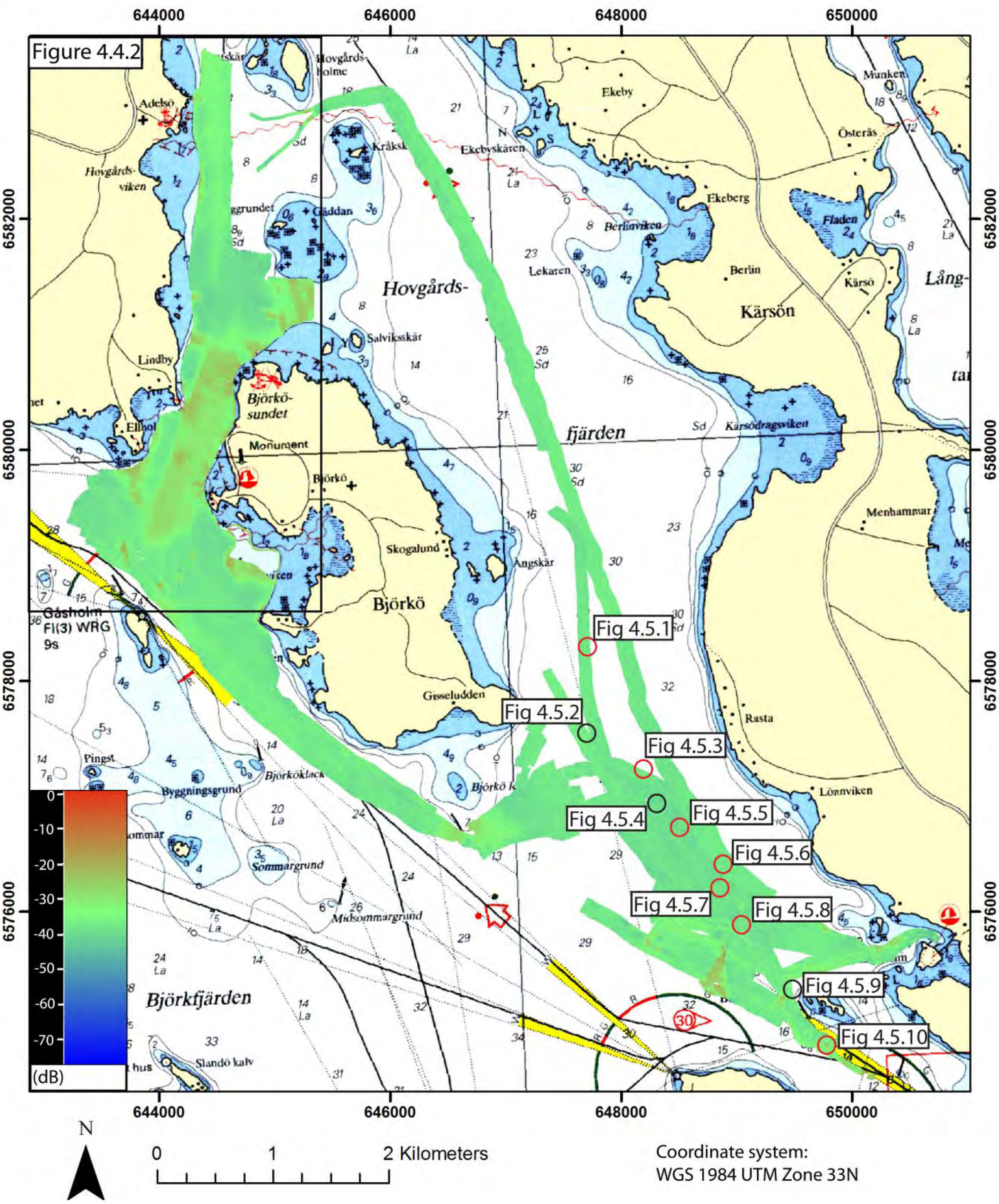

Figure 4.4.1. The backscatter result for the entire survey area. The backscatter values of Area 2 are relatively homogenous, generally in between -30 and -40 dB. Area 1 (marked by the black box) generally shows higher values – often around -20 dB. The numbered circles in the figure show the location for the BS objects in Area 2, which exclusively consists of shipwrecks. Nine of these wrecks are registered (red circles) and four are not (black circles). One of the unregistered shipwrecks is on the top of, or below the registered shipwreck represented by fig. 4.5.5. Therefore this unregistered shipwreck is not represented by a black circle here. Basemap is from Sjöfartsverket navigational chart: Mälaren – Östra delen.

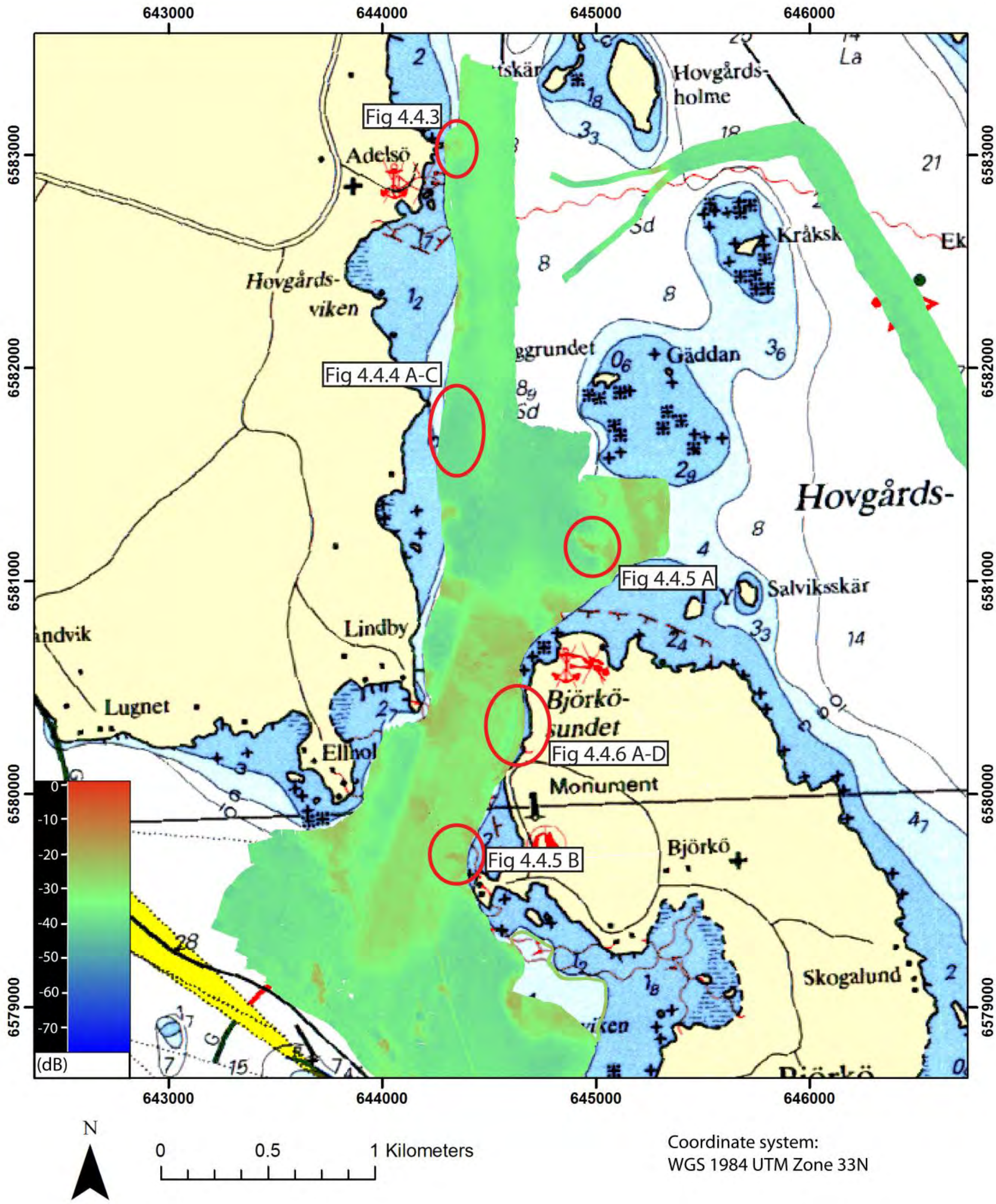

Figure 4.4.2. Shows the backscatter result of Area 1. The numbered circles/ellipses are highlighting the locations of the BS features that are presented in the text below. All these features correspond to objects from the multibeam bathymetry, except figure 4.4.6A-D which only is visualized here. Basemap is from Sjöfartsverket navigational chart: Mälaren – Östra delen.

BS feature 1

The high backscatter values in this division of the otherwise lower backscatter values have been divided into two different parts (fig. 4.4.3 A and B). Part A corresponds to ES object 1 (fig. 4.3.3A) and has a backscatter strength varying from -18 to -25 dB. Part B on the other hand varies in between -20 and -27 dB. The latter part of BS object 1 is barely visible in the multibeam bathymetry data. Possible reasons for this difference will be mentioned in the discussion.

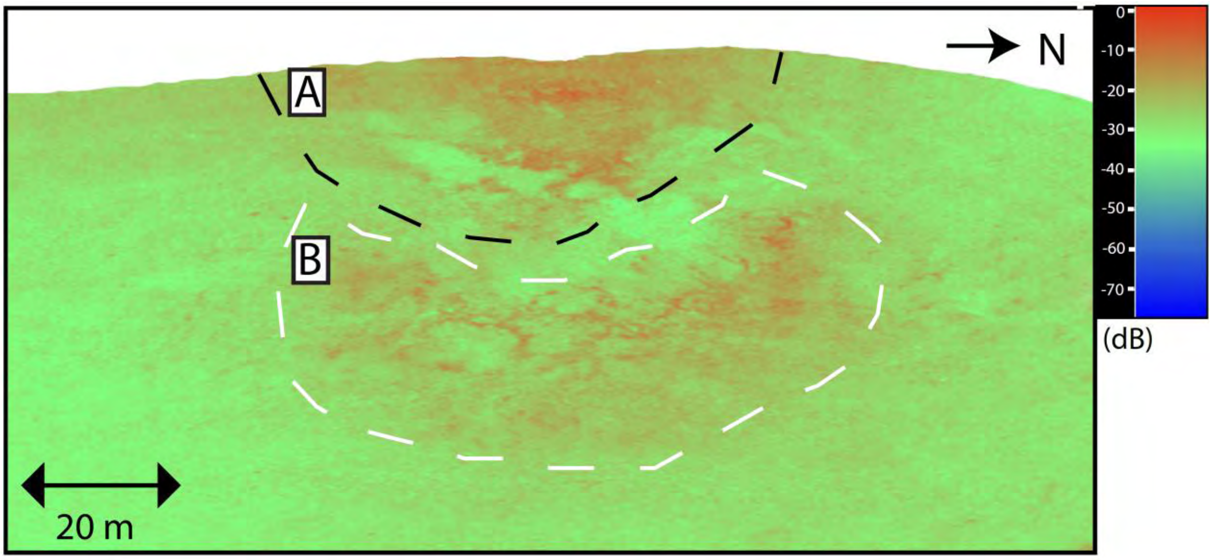

Figure 4.4.3. BS feature 1 is characterized by two areas of relatively high backscatter values (A and B). Part A of this BS feature corresponds to ES feature 1, while part B barely is visible in the multibeam bathymetry data.

BS feature 2

The three different objects that have been grouped together to BS feature 2 (fig. 4.4.4A-C) are the backscatter equivalents of the ES objects A, C and D in ES feature 2 (fig. 4.3.4). The three backscatter objects in this case show a higher backscatter strength (-30 dB) compared to the surrounding area (-40 dB). ES object 2B cannot be spotted in the backscatter data and is therefore not presented here.

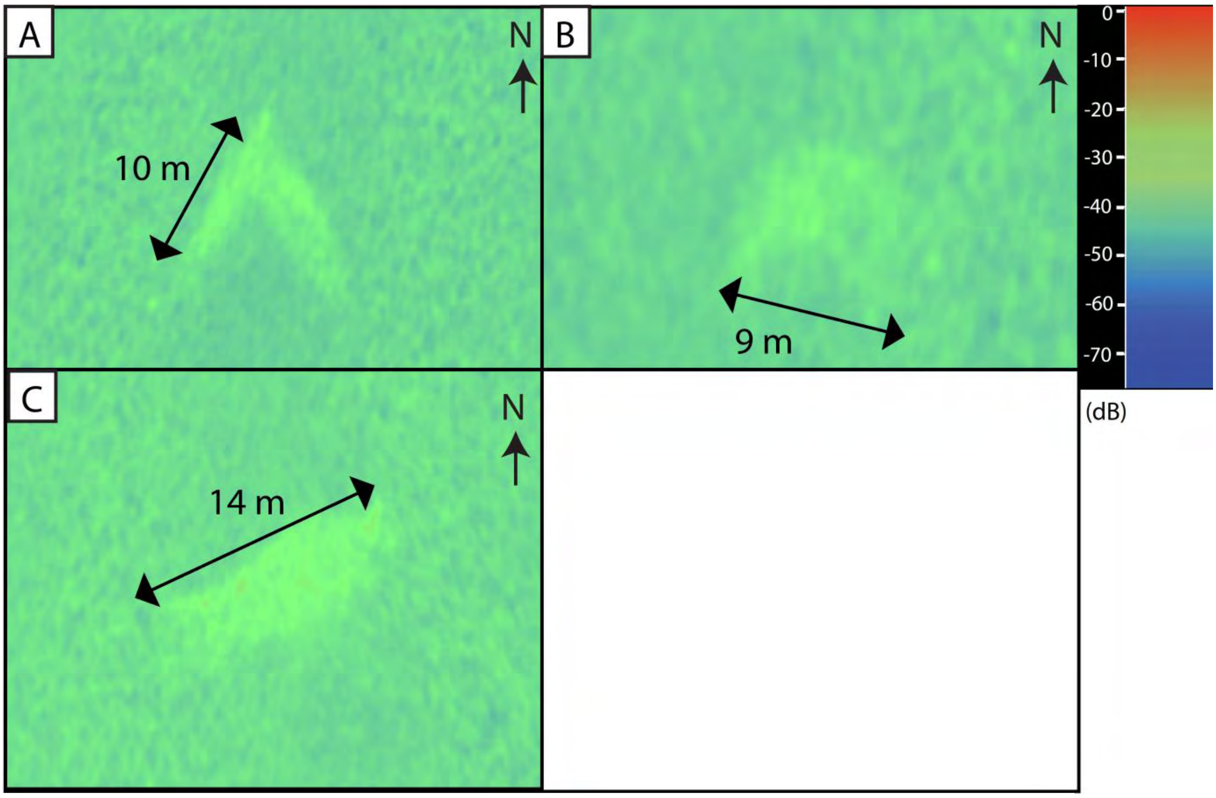

Figure 4.4.4. BS feature 2 shows the corresponding backscatter data of the ES objects 2A, C and D. ES object 2B could not be characterized in the backscatter data and is therefore not presented here.

BS feature 3

The ES objects that are included in ES feature 4 (fig.4.3.6A-D) appear in two different ways in the backscatter data which is presented in figure 4.4.5A and B below. These are the backscatter equivalents of figure 4.3.6A and 4.3.6C respectively.

Figure 4.4.5A indicates relatively high backscatter values (-14 to -20 dB) for the elevated bathymetry (red) surrounding the pointy objects. On the other hand, the pointy objects on top have significantly lower backscatter values – sometimes as low as -50 dB (blue/green dots). This relation is representative for all the objects grouped into ES feature 4, except in the case of ES object 4C (fig 4.3.6C). In this case the pointy objects have similar backscatter values (around -20 dB) as the elevated bathymetry surrounding it (fig.4.4.5B).

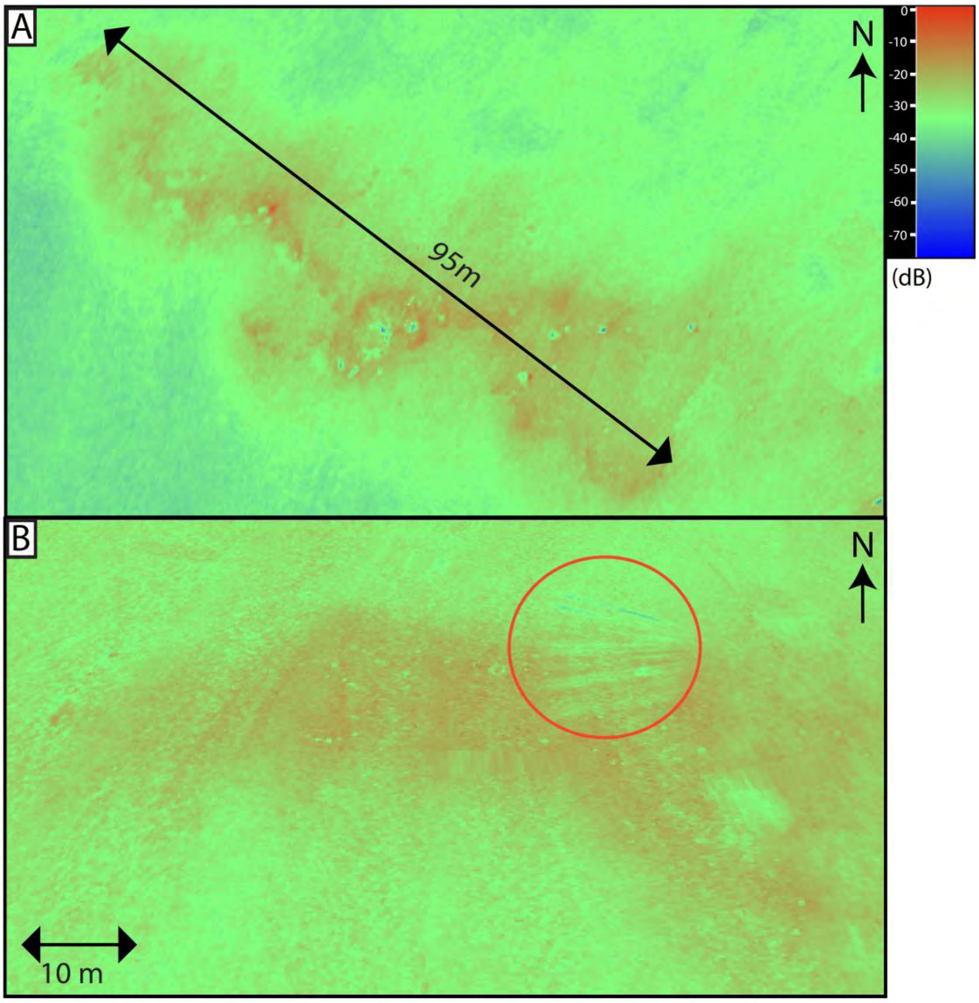

Figure 4.4.5. BS feature 3 shows the two different ways (A and B) that the ES feature 4 responds to the backscatter data. Case A is the most common response, where the backscatter values of the pointy objects (blue/green) are significantly lower than the surrounding bathymetry (red). In case B the backscatter values of the pointy objects are similar to the surrounding bathymetry (red). The parallel stripes of relatively low backscatter values indicated by the red circle in B are noise in the data and should not be considered.

BS feature 4

Figure 4.4.6A-D is examples of BS objects from the former harbor area of Birka. Most of the objects in this area look like the examples with the white length scales in figure 4.4.6A, B and D. To the shape these unidentified objects are all straight and have lengths that usually vary in between 2 and 4 m and widths from 0.6 to 0.7 m. Their backscatter values reach from -25 to -30 dB.

The circular object in figure 4.4.6A together with the object in 4.4.6B are the only two identified objects from this are that does not fit in to the latter description. Case A can instead be described as a circular object with a diameter of 1.4 meters. Its minimum backscatter strength is -40 decibel. Case C is similar to the straight and unidentified objects regarding length and shape, but is wider and curvier and also has a lower backscatter strength (-32 dB).

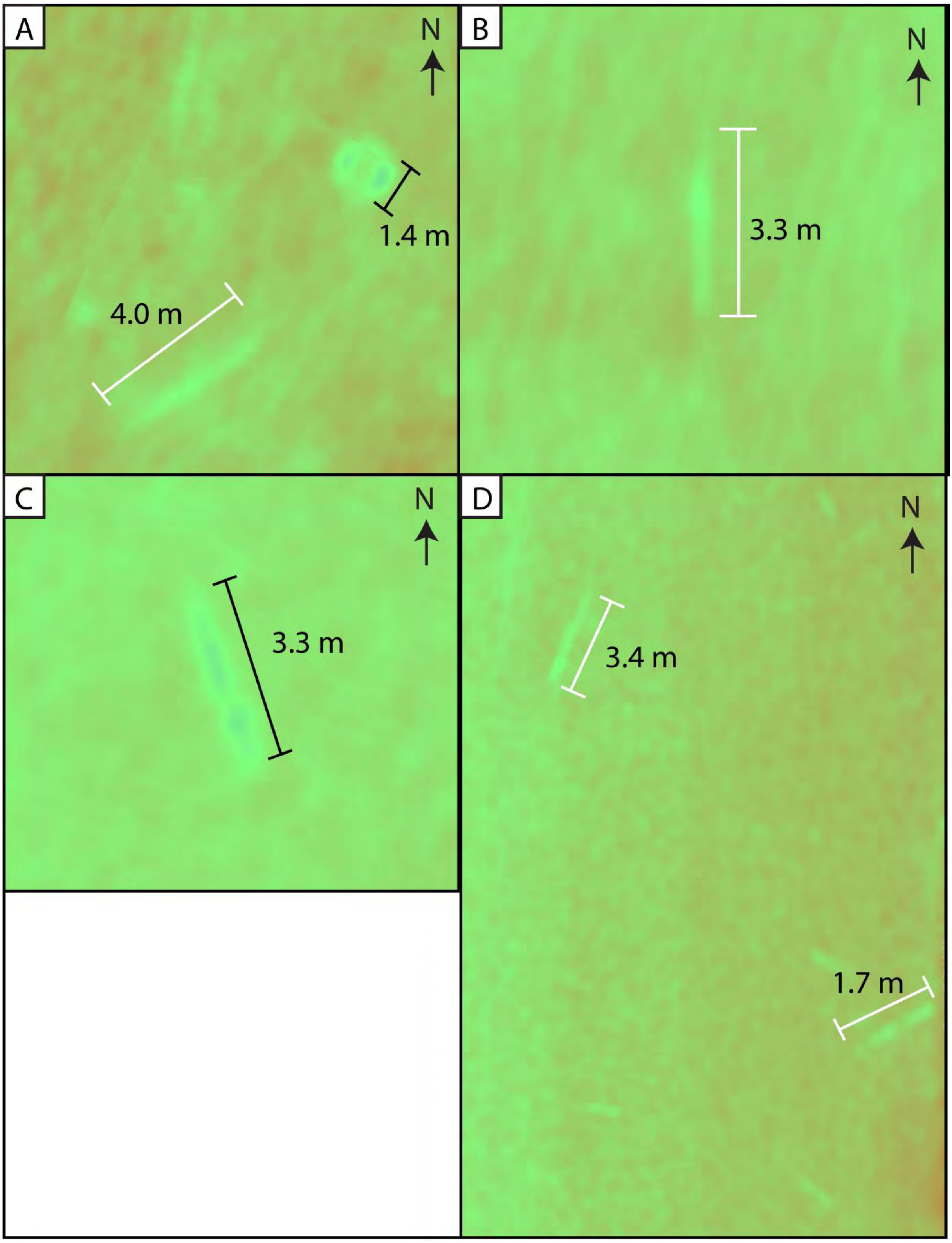

Figure 4.4.6. BS feature 4. Examples of BS objects from the former harbor area of Birka. This area is characterized by elongated objects with lengths in between 2 and 4 m and widths from 0.6 to 0.7 m similar to the objects with the white length scales in A, B and D. The circular object in A and the elongated, but curvier object in C have unique shapes.

4.5 Shipwrecks

The BS objects found in Area 2 (fig. 4.4.1) exclusively comprise shipwrecks. These shipwrecks have been matched with the shipwrecks registered in “Fornsök” by “Riksantikvarieämbetet (Swedish National heritage board). Fornsök is a data base containing information about all types of known ancient monuments and relics spread across Sweden - both on and offshore. There are no special requirements for a shipwreck to be registred in Fornsök. Fornsök comprise all types of wrecks from smaller boats to larger ships, no matter their age. Each shipwreck registered in Fornsök has an individual identification number, called RAÄ number.

In the survey area covered by this thesis, 13 shipwrecks have been found. Their respective locations are marked by numbered ellipses/circles in figure 4.4.1. Of the 13 shipwrecks, nine are registered in Fornsök. The individual RAÄ numbers will be presented for these shipwrecks together with their respective coordinates (WGS 84 UTM zone 33 N) and observations done in the gridded data sets. The four unregistered shipwrecks are naturally not confirmed, but will still be treated as shipwrecks here due to their suitable dimensions in the bathymetry and appearance in the backscatter data.

Shipwreck 1

This is a confirmed barge vessel (RAÄ number: Adelsö 188) that lies on an approximate depth of 23 m (fig. 4.5.1). The ship wreck is well preserved and has been examined by divers who concluded that the cargo consists of rice and “garbage” (Fornsök, 2012-10-04). The dimensions of this barge vessel are about 25×12×3 m.

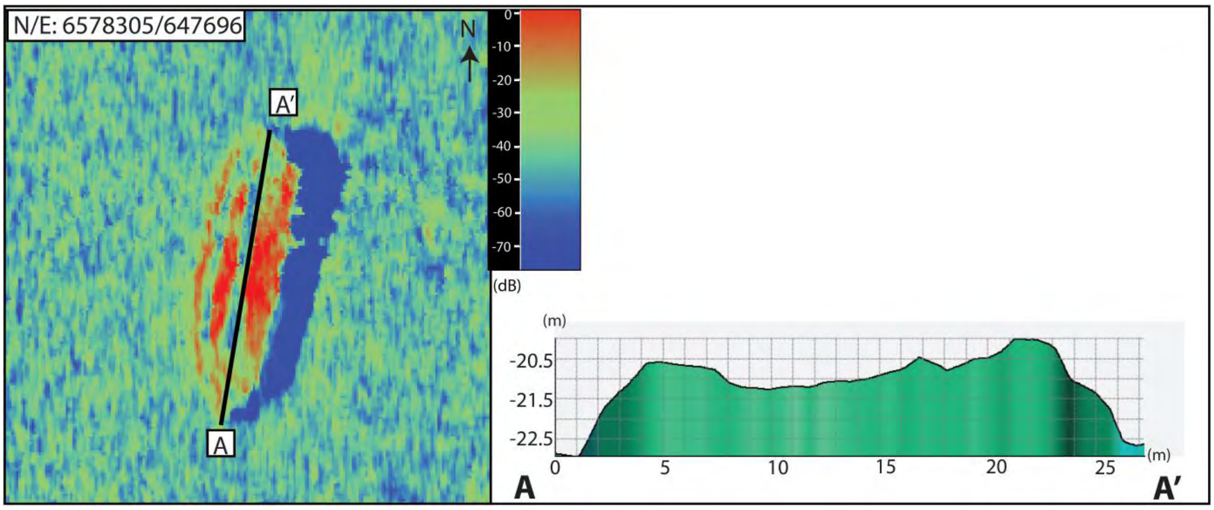

Figure 4.5.1. The registered barge vessel ”Adelsö 188” (left) and its cross cutting profile (right).

Shipwreck 2

This BS object is about 20 m long and 7 m wide and was spotted on an approximate depth of 30 m (fig. 4.5.2). It has not been confirmed by the shipwreck register. This BS object is only visible in the backscatter data, but not in the multibeam bathymetry data. This observation will be discussed further on.

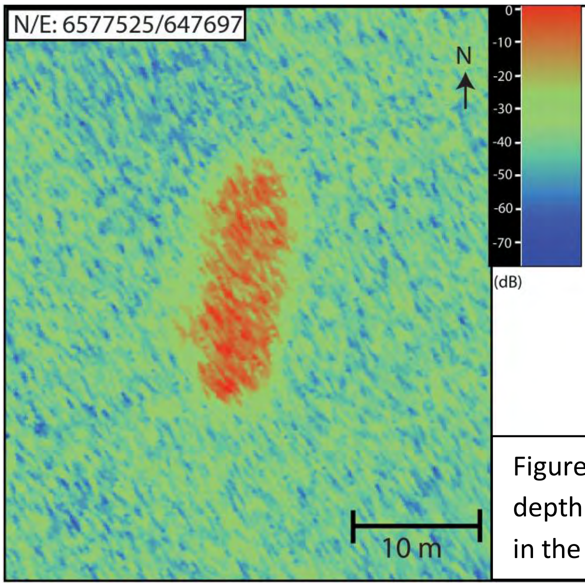

Figure 4.5.2. An unidentified BS object on 30 meters depth that only is visible in the backscatter data but not in the bathymetry.

Shipwreck 3

This shipwreck is around 8 m wide and is situated on a depth of approximately 30 m (fig. 4.5.3). A closer description is not possible since parts of this object are missing due to the location at the edge of the dataset. Clear is that there is a registered shipwreck on this location with the RAÄ number Ekerö 243. Probably it is a barge vessel that due to the weak signal either is partly covered by sediment or is relatively degraded (Fornsök, 2012-10-04).

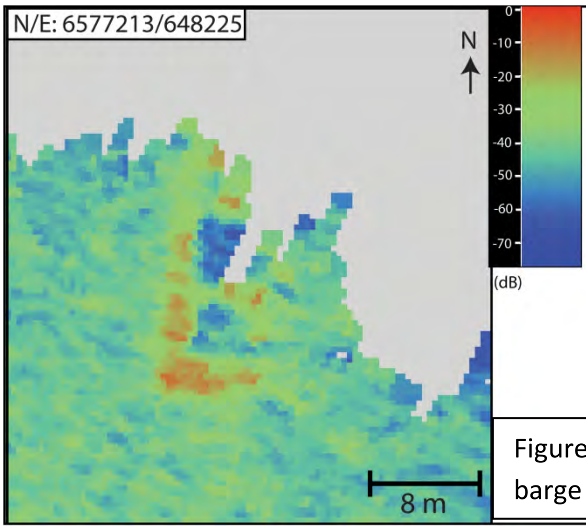

Figure 4.5.3. A low quality picture of the registered barge vessel with RAÄ number Ekerö 243.

Shipwreck 4

This BS object is not confirmed in the shipwreck register, lies on a depth of about 31 m and has the approximate dimensions of 23×13×1.6 m (fig. 4.5.4). It should however be noted that this shipwreck has been confirmed and reported before. Why it is not in the register is unknown (Flood, personal communication).

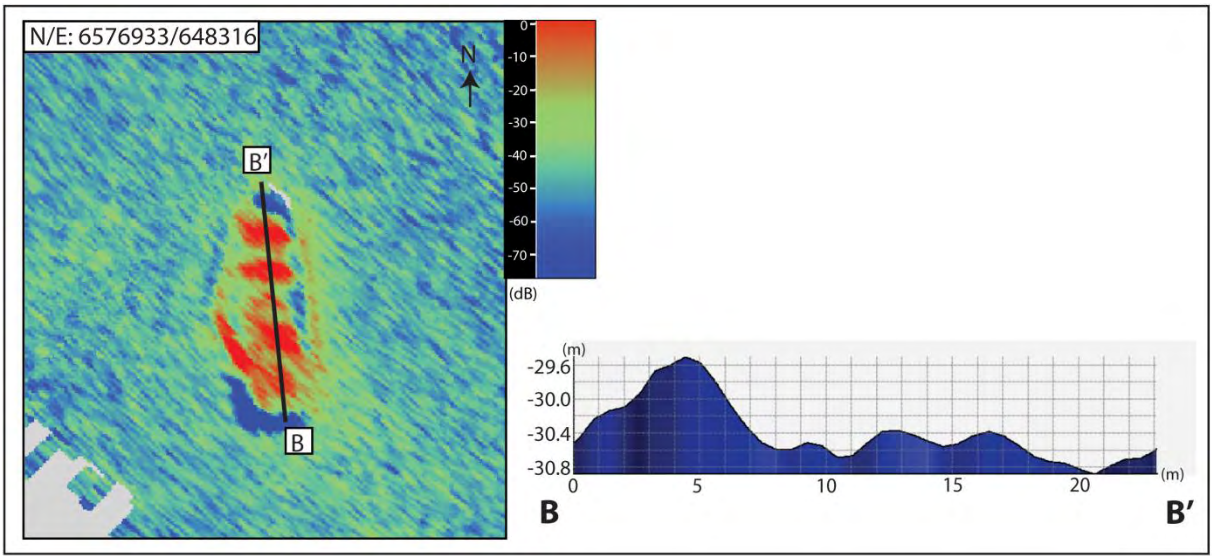

Figure 4.5.4. An unregistered BS object on 31 m depth (left). Its crosscutting profile (right) clearly reminds of a barge vessel.

Shipwrecks 5, 5X and 6

At first only the two shipwrecks with corresponding crosscutting profiles were spotted in this area (fig.4.4.5). These two BS objects are both registered shipwrecks on an approximate depth of 30 m. No diving has been done here so more specific information is not available, but probably both objects are barge vessels (Fornsök, 2012-10-04). The respective RAÄ numbers for these wrecks are Ekerö 247 (Object 5, northernmost in figure 4.5.5) and Ekerö 235 (object 6, southernmost in figure 4.5.5) (Fornsök, 2012-10-04). The dimensions of Ekerö 247 are 22×8×3.5 m, while Ekerö 235 has the dimensions of 21×7×2.5 m.

When the bathymetry covering this area was studied more carefully a third shipwreck was spotted situated under what in figure 4.4.5 is shipwreck 5. Since the new shipwreck shares the same coordinates with shipwreck 5, it is unknown which of them the register refers to. The new shipwreck is therefore from now on referred to as “Shipwreck 5X”. Shipwreck 5X is better visualized in the upcoming 3D model for the actual area (fig. 4.6.1).

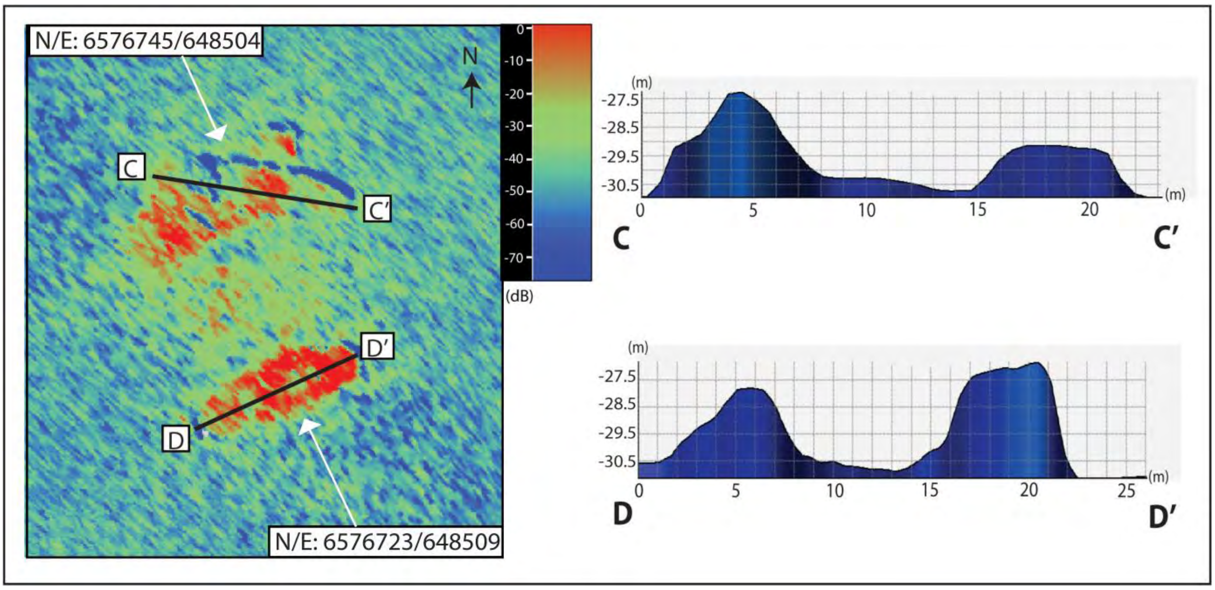

Figure 4.5.5. The two registered shipwrecks Ekerö 247 (northernmost in the left figure) and Ekerö 235 (southernmost in the left figure) and their respective cross cutting profiles to the right. A third shipwreck was spotted below what in this text is Ekerö 247. Since Ekerö 247 has the same coordinates as the new shipwreck, it is here unsure which one of these two wrecks the register refers to. The new shipwreck is therefore referred to as "Shipwreck 5X", and is better visualized in the 3D model of the bathymetry that covers this area (fig. 4.6.1).

Shipwreck 7

This is a registered shipwreck (RAÄ number: Ekerö 228) (Fornsök, 2012-10-04), with the dimensions of 21×7×2 m and rests on an approximate depth of 28 m (fig. 4.5.6)

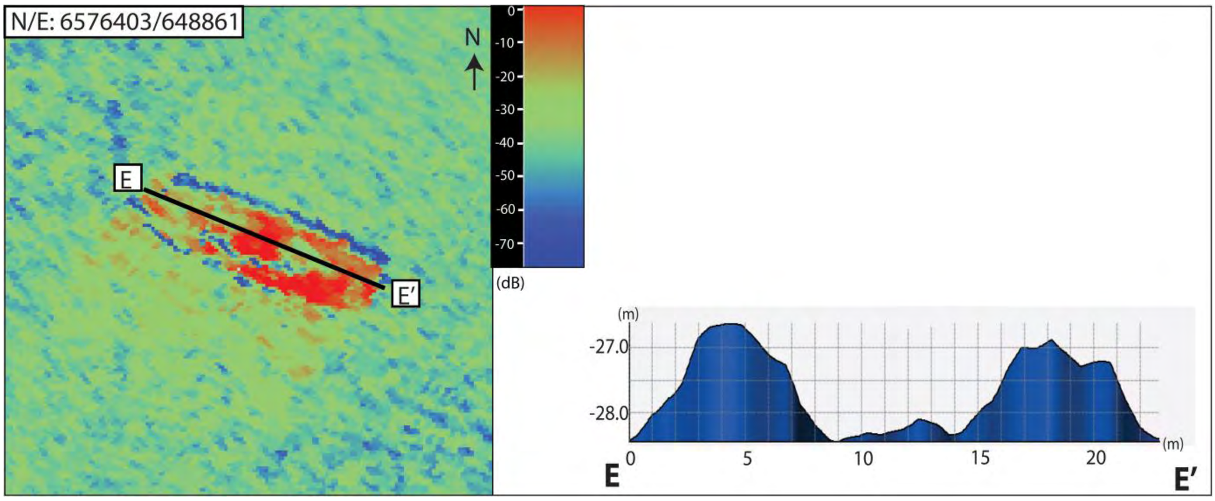

Figure 4.5.6. The registered shipwreck "Ekerö 228" (left) and its cross cutting profile (right).

Shipwrecks 8 and 9

The respective RAÄ numbers for these two registered shipwrecks are “Ekerö 231” (westernmost in figure 4.5.7) and “Ekerö 232” (easternmost in the figure 4.5.7). Both the wrecks are probably barge vessels (Fornsök, 2012-10-04), and their dimensions are approximately 24×8×1.4 m (Ekerö 231) and 22×8×2.2 m (Ekerö 232).

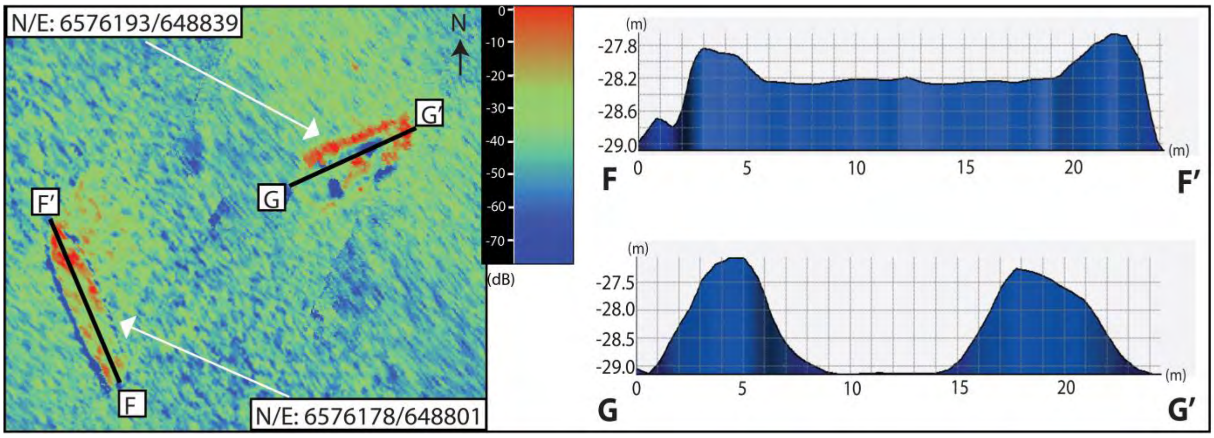

Figure 4.5.7. The two registered shipwrecks Ekerö 231 (westernmost in the left figure) and Ekerö 232 (easternmost in the left figure) and their respective cross cutting profiles below.

Shipwreck 10

This is a registered barge vessel (RAÄ number: Ekerö 225) with the approximate dimensions of 23×7.5×0.6 m (fig. 4.5.8). The cargo is filled with sediment but the ship is otherwise intact where it lies on a depth of 29 m (Fornsök, 2012-10-04).

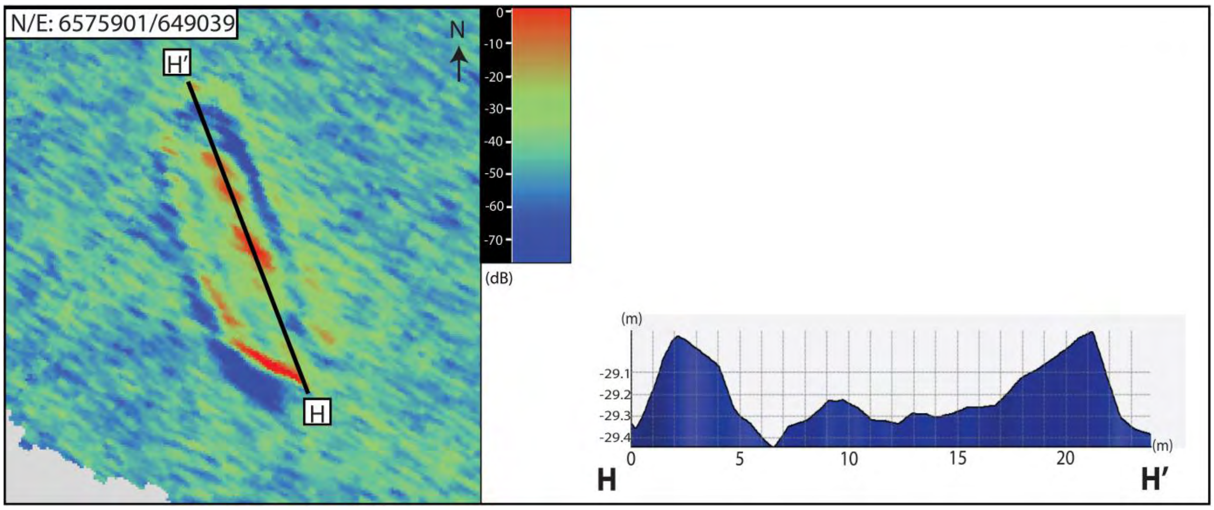

Figure 4.5.8. The registered shipwreck “Ekerö 225” (left) and its cross cutting profile (right).

This BS object was found on an approximate depth of 20 m and is not a found in the shipwreck register. Its dimensions are approximately 13×3×1.3 m (fig. 4.5.9), which are relatively different from the previously presented registered wrecks.

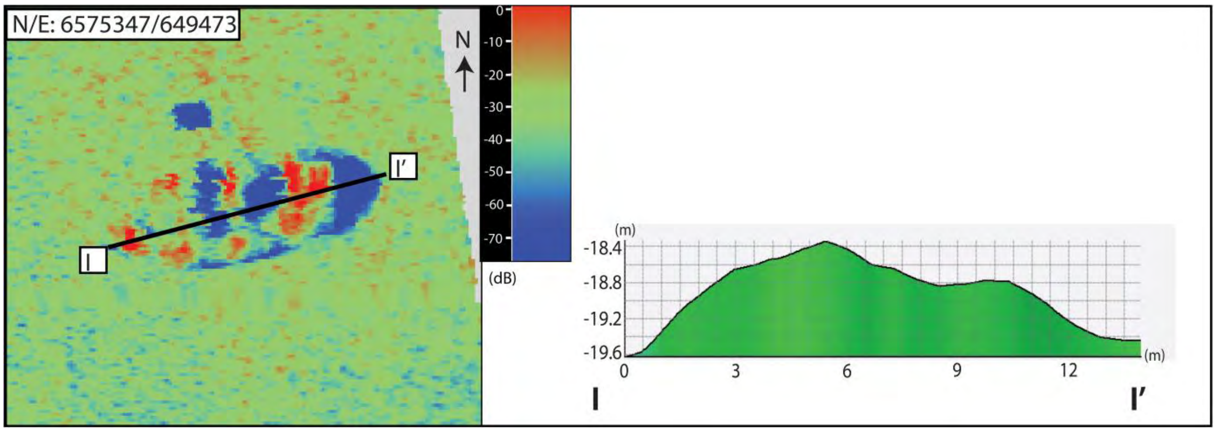

Figure 4.5.9. An unregistered BS object (left) with relatively different dimensions (right) compared to the previously confirmed wrecks.

Shipwreck 12

This is a registered barge vessel called "Marjaana" (RAÄ number: Ekerö 208) which history is well known (fig. 4.5.10). The ship has the approximate dimensions of 37×9×5 meters was built in 1944 and consisted mostly of concrete which was an experiment construction at that time. The sinking of Marjaana took place in the year of 1969 when the ship collided with ice on the lake. Even though the sinking went relatively fast, everyone in the crew except a dog survived. Today the ship is located on a depth of 15 m (Fornsök, 2012-10-04).

In addition to the shipwreck, there is also an area reaching about 10 meters to the south from the shipwreck that emits a significantly high backscatter signal compared to its surroundings. This area is represented by grain sizes varying from sand to gravel in the ARA data and is relatively easy to detect since it covers the clay dominated lake floor (fig. 4.5.10).

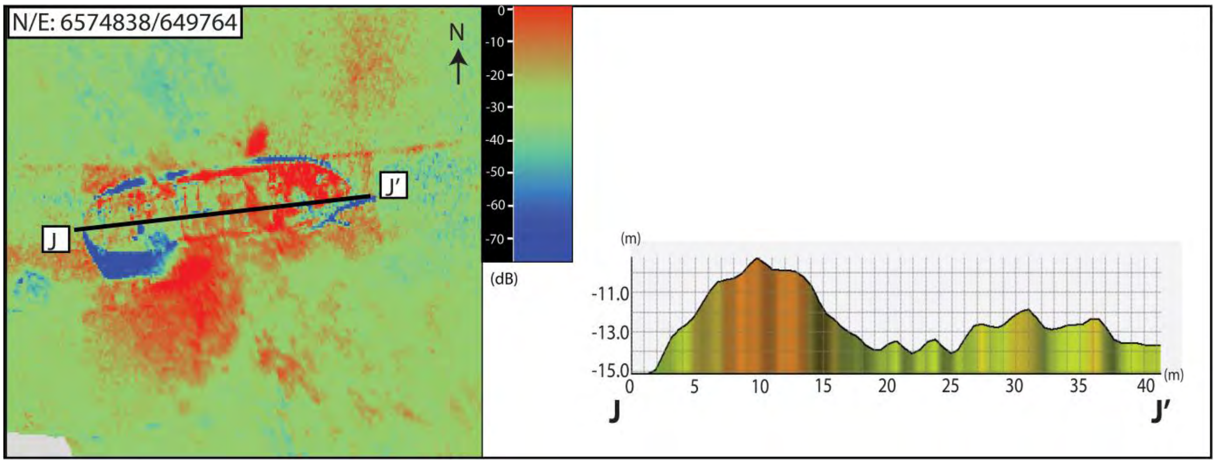

Figure 4.5.10. The confirmed shipwreck "Marjaana" (left) and its cross cutting profile (right).

4.6 3D models of shipwrecks

To give another perspective of the shipwrecks presented in the backscatter data, five of them are below shown as 3D models from the multibeam bathymetry data. Which shipwreck from the backscatter data the actual 3D model corresponds to will be clear in the text. Before the presentation it should be stated that the quality of the presented 3D models varies depending on the resolution, which is why the figures 4.6.1 and 4.6.2 less detailed than figure 4.6.3.

3D model 1

Figure 4.6.1 shows the 3D models for the shipwrecks 5, 5X and 6 presented in the backscatter data (fig. 4.5.5). In this 3D model, the unregistered shipwreck 5X can easier be spotted, lying either below or above shipwreck 5. These two shipwrecks are situated to the North in figure 4.5.5, while shipwreck 6 is found in the South.

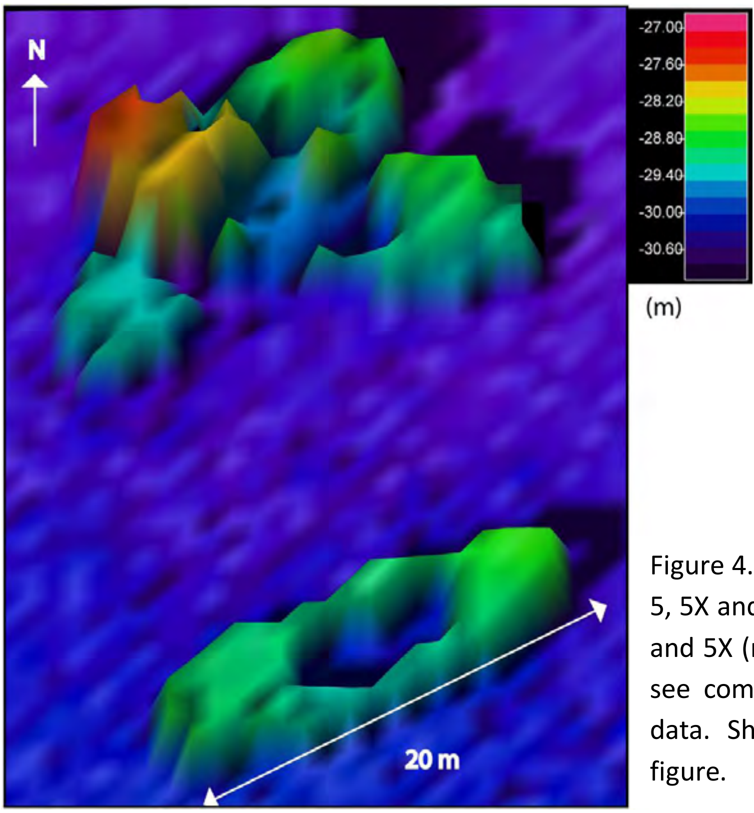

Figure 4.6.1. 3D model of the backscatter shipwrecks 5, 5X and 6. The relation in between the shipwreck 5 and 5X (northernmost in the figure) is here easier to see compared to in the corresponding backscatter data. Shipwreck 6 is found southernmost in the figure.

3D model 2

Figure 4.6.2 corresponds to the unregistered BS object shipwreck 11 (fig. 4.5.9). As mentioned this object has relatively different dimensions compared to the majority of the registered wrecks and is more similar to a speed boat than a barge vessel (fig. 4.6.2).

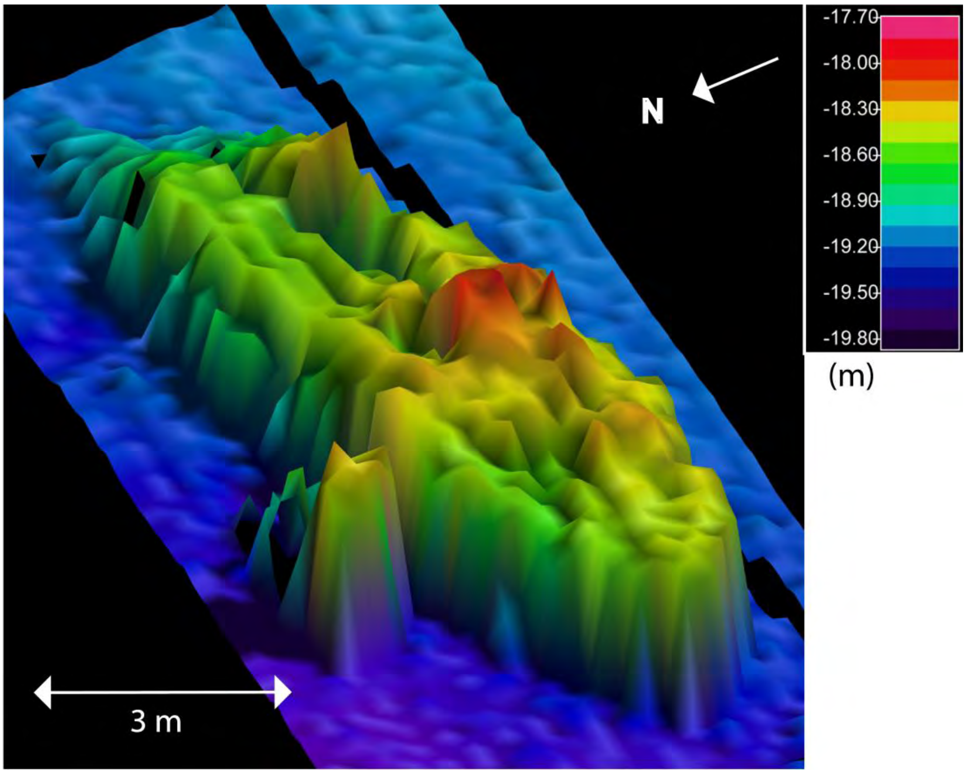

Figure 4.6.2. 3D model of the unregistered backscatter shipwreck 11. Here it is easier to see that the actual shipwreck has relatively different dimensions compared to the majority of the registered shipwrecks more similar to a speed boat than a barge vessel.

3D model 3

Figure 4.6.3 shows a high resolute 3D model corresponding to shipwreck 12, which is the registered barge vessel “Marjaana” (fig. 4.5.10).

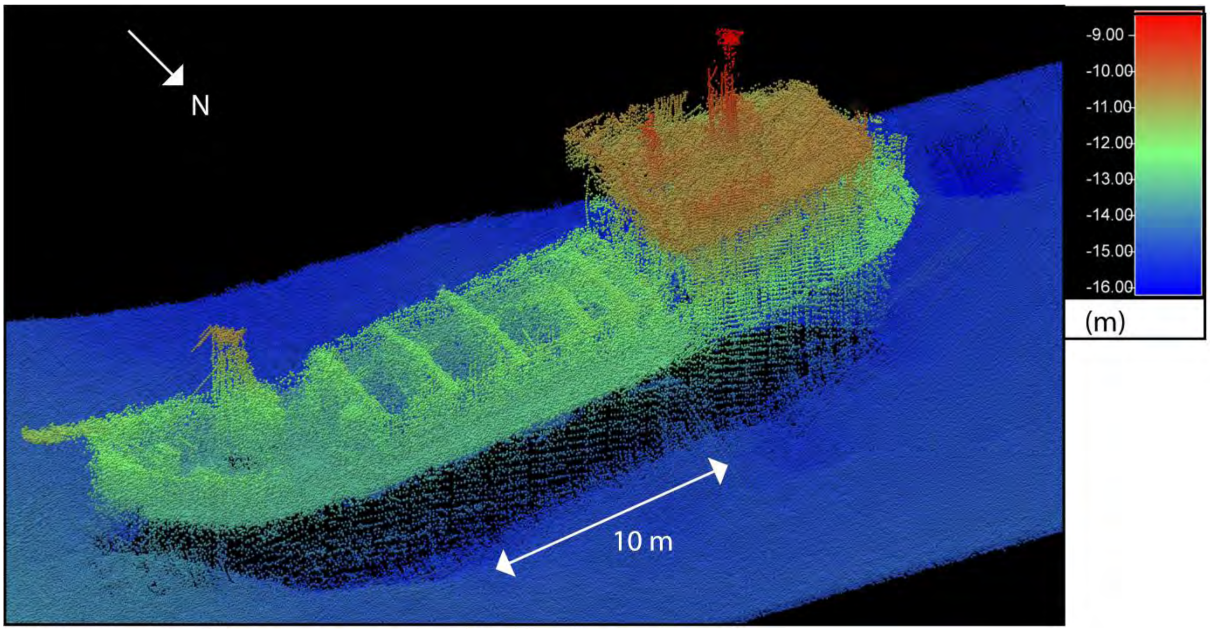

Figure 4.6.3. 3D model of the registered shipwreck “Marjaana”.

4.7 Angular range analysis

The angular range analysis indicates that the most dominant grain sizes of the sediment types exposed at the lake floor in the study area are clay to fine silt, but grain sizes all the way up to gravel are present (fig. 4.7.1). Similar to the backscatter result, Area 1 is also here the most heterogenic area. Sand is dominating the strait in between Adelsö and Björkö.

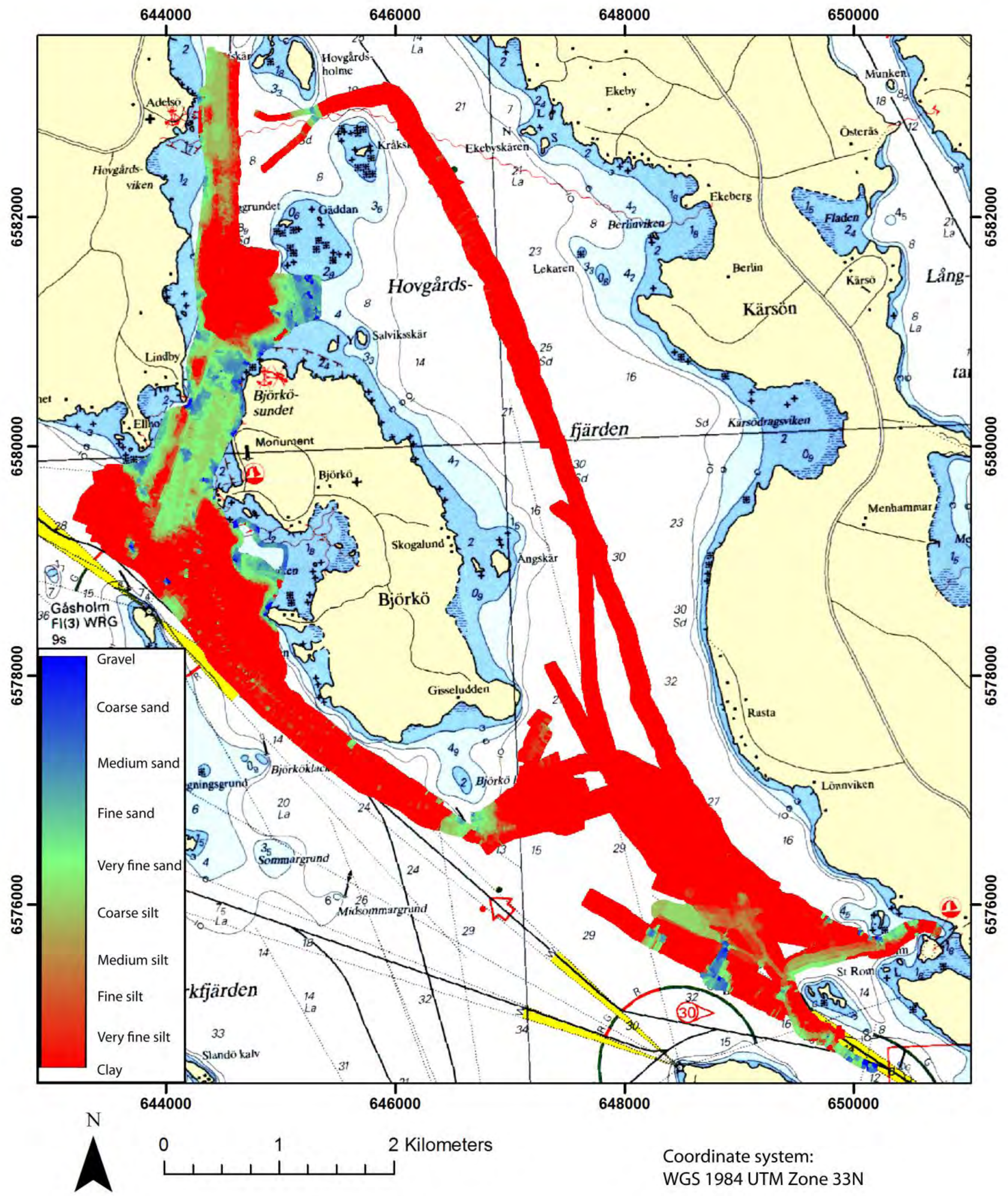

Figure 4.7.1. The ARA result for the total study area suggests that clay to fine silt are the most common grain sizes of the sediment on the lake bottom. Area 1 shows a greater range of grain size heterogeneity than Area 2. Basemap is from Sjöfartsverket navigational chart: Mälaren – Östra delen.

5. Discussion

5.1 Interpretation of the acoustic sediment units

As mentioned in the introduction, the modern Baltic Sea has gone through several stages during the last 12600 cal yr BP. The different depositional environments that have been coming and going during these stages have all had their own impact on the sediment stratigraphy of the Baltic Sea (Björck, 1995).

The aim with this part of the discussion is to correlate the acoustic sediment units with the different stages that have existed from the Baltic Ice Lake until the modern Baltic Sea. This correlation is in the theory possible until the isolation of Lake Mälaren, which happened in between 1000 and 1300 AD (Risberg et al., 2002). There are no sediment cores available from this study to correlate the acoustic stratigraphy with. This means that it is not possible to verify the interpretation of the acoustic units. However, Risberg and Björck (1997) carried out a lithostratigraphic study in the harbor area of Birka where sediment cores were obtained using a Russian corer. In the results from the coring by Risberg and Björck (1997) it was stated that the sediment stratigraphy generally can be described as seen in table 5.1.1, where the sediment type in the bottom is the oldest and the one in the top is the youngest.

Sediment type	Maximum thickness (cm)	Other	Time of deposition
Clay gyttja	-	Wood fragments and charcoal particles	Post-Birka time
Organic rich	-	Black soil	Tentatively Birka time
Silty clay	-	-	Tentatively Birka time
Gyttja clay	108	-	Littorina Sea
Grey clay	200	-	Yoldia Sea-Ancylus Lake
Brownish clay	265	-	Yoldia Sea-Ancylus Lake
Sandy clay	100 (stops at coarse material)	Often containing gravel	Yoldia Sea-Ancylus Lake

Table 5.1.1. The sediment stratigraphy in the harbor area of Birka can generally be described according to this table, where the sediment type in the bottom is the oldest while the one in the top is the youngest. Modified from Risberg and Björck (1997).

The three clay layers in the bottom of table 5.1.1 are not accurately correlated to a specific stage of the Baltic Sea basin. Still table 5.1.1 is important for the local sediment stratigraphy of the study area. Therefore it may be valuable for the correlation of the acoustic units (U1-U5) from this study with the stages of the Baltic Sea basin (table 5.1.2). This correlation is presented below.

Stages of the Baltic Sea basin	cal yr BP.	Characteristics of the sediments
The Baltic Sea	3000-present[2]	Gyttja clay and anoxic bottom conditions [5,8].
The Littorina Sea	9800-3000[2]	Gyttja clay and anoxic bottom conditions [5,8].
The Ancylus Lake	10700-9800[3]	Homogenous clay[7].
The Yoldia Sea	11600-10700[2]	Varved glacial clay. The varves get weaker the further from the retreating ice margin it is deposited[5,6].
The Baltic Ice Lake	12000-11570[1]	Varved glacial clay. The varves are prominent due to deposition close to the retreating ice margin[4].

[1]Andrén et al., 2000 [2]Björck, 2011 [3]Andrén et al., 2011 [4]Ignatius, 1958
[5]Ignatus et al., 1981 [6]Hutri and Kotilainen, 2006 [7]Björck et al., 1996 [8]Risberg and Björck, 1997

Table 5.1.2. The stages of the Baltic Sea basin influenced by the retreat of the Late Weischelan ice sheet. Next to each individual stage are the age (in cal yr BP) presented together with the dominating sediment type.

U1. The prominent repetitive internal reflectors that build this unit indicate that the sedimentation during this time was rhythmic and thus controlled by some kind of regular forcing. The appearance of this unit is recognized from several previous published results (table 5.1.2) and is here proposed to consist of glacial clay. This hypothesis is supported by Flodén et al., 1993, who carried out mapping of the sediment stratigraphy in Björköfjärden, south of Björkö, and concluded that what is U1 in this thesis equals glacial clay.

The varves in glacial clay are formed due to the yearly cyclical pattern in between melting and less or no melting of the glaciers. During summer time when the grade of melting is relatively high, the melt-water brings larger quantities of coarser grained sediments compared to the cooler winter time when the melt water ceases. This leads to regular varves in the accumulating glacial clay that is deposited in fresh or brackish water. The coarser grained sediments gives thicker varves, with a lighter color compared to the thinner and darker winter varves mainly consisting of clay. The varves of the glacial clay are more prominent the closer to the ice margin they are deposited (de Geer, 2002).

It should be stated that it is not the individual varves that are seen in the acoustic profiles from the subbottom profiles. Instead, it is the rhythmical impedance contrasts which are formed when the sound pulse is travelling through the glacial clay that together cause the regular reflections that are visualized (Jakobsson, personal communication).

The acoustic characteristics of the sandy clay containing gravel (table 5.1.1) would probably give similar prominent and repetitive internal reflectors as U1 does. Therefore it is likely that these units can be correlated. The sandy clay (table 5.1.1) could not be fully penetrated and its thickness can therefore not be compared to the one of U1. When trying to correlate U1 to a specific stage of the Baltic Sea basin, it has probably been deposited during the early Yoldia Sea stage. These deposits could not have been formed during the Baltic Ice Lake since this area still was covered with ice at that time (Björck., 1995).

U2. U2 is likely to have been deposited in a transition period from a glacial dominated to a non-glacial dominated time. This is suggested since U2 shows similar acoustic characteristics as U1, but with weaker internal reflectors following the same pattern as the ones in U1. This indicates that the rhythmical change of the coarse grain component is still present in the clay, but that the ice margin has retreated further away from the depositional area and thus gives a weaker imprint in the stratigraphy.

The U2 unit may therefore have been deposited during the late Yoldia Sea stage or during the Ancylus Lake stage. During these stages, the Late Weischelan ice sheet that dominated during the Baltic Ice Lake had retreated further north. This may have lead to a relatively low energy depositional environment in the study area. In turn, this resulted in glacial clay with finer laminations than during the Baltic Ice Lake stage (table 5.1.2). This may be indicated by the internal reflectors of the U2 unit. It is therefore probable that U2 corresponds to the brownish and grey clays, which together have a maximum thickness of 4.65 m (table 5.1.1). This thickness is relatively close to the maximum thickness recorded for U2, which is 5.0 m.

U3. The internal reflectors of this unit are not sharing the acoustic characteristics with the previous units. Therefore it is here suggested that U3 is not comprised of rhythmically deposited clay. This may exclude that U3 would consist of varved clay. It should however be noted that there is a grade of uncertainty here, since there might be varves in this unit that are not visible in the acoustic profiles.
However, the thick and sharp reflector between U3 and U2 indicates that there is an abrupt change in sediment density, which also can be assumed from the erosion patterns where U3 often (especially in Area 2) is lacking while the previous units still remain. The limited extent of the U3 unit in Area 2 may also indicate that there is and has been more current activities here compared to in Area 1. This may depend on that Area 1 is more protected from currents in the relatively shallow strait in between Adelsö and Björkö.

U3 might be dominated by gyttja clay, which was a common sediment type during the Littorina Sea stage (table 5.1.2). The maximum thickness of the gyttja clay in table 5.1.1 is 1/3 of the maximum thickness recorded for U3. This could be explained by the different data locations where the coring in table 5.1.1 was done relatively close to the shore where the sediment stratigraphy may be thinner.

U4. U4 was described as a surficial unit consisting of loose sediments that are being deposited at the moment. This could seem somewhat inconsistent since U4 does not appear as a single unit in between two reflectors as in all the other cases. However, U4 cannot be described as a single reflector because it is too thick. Also the fact that the thickness varies depending on location tells that this is a unit and not a single reflector. U4 could therefore possibly be the post-Birka top unit consisting of clay gyttja and wood fragments as described by Risberg and Björck (1997).

U5. This unit was found as four individual areas within Area 1 that acoustically look the same – semitransparent units that lack internal reflectors. The only visual difference between the four areas of U5 is that one of them covers a significantly bigger area and volume compared to the other three. From now on, focus will be put on the biggest of the four U5 areas which also coincides with the location of the "Type 1 point objects"

The origin of the Type 1 point objects cannot be verified in this thesis. This depends on the significant difference in visualization of the "Type 1 point objects in between the data from the subbottom profiler and the multibeam bathymetry echosounder respectively. This difference together with the sometimes relatively even distribution of the type 1 point objects in the U5 acoustic unit leads to three main hypothesizes of the origin of the type 1 point objects and its relation to U5.

In the first hypothesis, it is stated that the U5 unit is a highly organic sediment unit that produces gas. This is supported by two factors. Firstly, the transparency of the U5 unit and the lack of internal reflectors tell that this is a homogenous unit of relatively low density – maybe due to a high content of organic matter. Secondly, the transparency of the type 1 point objects may indicate that these objects are gas being emitted from the lake floor. This would explain why the majority of these gas columns and the U5 unit are found in the same area, and why the type 1 point objects are not visualized in the same way in the multibeam echo sounder data as in the subbottom profiler data. The latter data type has in previous studies been used for detecting gas seepages (von Deimling and Papenberg, 2012). Confirmed gas seepages similar to the possible ones in this case have for example been presented in Canet et al., (2010) and Hovland (2007).

Gas being emitted from the lake floor is generally in subbottom data connected to gas rich sediment found below the gas emission (Hutri and Kotilainen, 2007). The acoustic profile SBP 15161846 (fig. 4.1.2) in this thesis is a prominent example where the gas is disturbing the acoustic character of U1. This phenomena is absent in the sediment column below the type 1 point objects which therefore is a disproof regarding the first main hypothesis.

Therefore, there is a second main hypothesis for the relation in between U5 and the type 1 point objects. Here it is stated that U5 still is an organic rich sediment unit, while the type 1 point objects are some type of seaweed. This may explain the transparency of U5 and why the type 1 point objects behave differently in the subbottom data from the multibeam data. The organic rich U5 unit may also be of significance for the seaweed to grow, which would explain the relation in between U5 and the type 1 point objects. What it does not explain is the relatively even distance between four of the type 1 point objects (fig. 4.2.1 box A).

In the third and last main hypothesis it is stated that the type 1 point objects are manmade while U5 may be an anthropogenically affected sediment unit. The proofs for this idea are based on the relatively even distance in between four of the type 1 point objects within the U5 unit (fig. 4.2.1 box A). This may indicate that the point objects have been put there on purpose.

The disproof in the third case is the already mentioned difference in appearance of the type 1 point objects in between the data from the subbottom profiler and the multibeam bathymetry echosounder respectively. On the other hand, the multibeam bathymetry echosounder data may not be optimal for studying the type 1 point objects. Therefore it is here suggested to study the water column data from the multibeam sonar which may show the type 1 point objects from another perspective.

5.2 Comparison of the acoustic sediment units with the angular range analysis

The acoustic units from the subbottom data together with the ARA data are interpretations of the nature of the sediment. The acoustic units are made from visual interpretations while the ARA is mathematically calculated. Correlating the interpretations from the acoustic units exposed at the lake floor with the ARA result can therefore be interesting. Firstly, a relatively good correlation in between the two data sets would support the interpretation of the acoustic units. Secondly, a good correlation may hint about the grain size of the acoustic units, which is a physical property that the subbottom profiler alone cannot collect. Such a correlation could therefore support the interpretation of the acoustic units presented above.

Therefore, a comparison between the areal distribution of the acoustic units on the bottom surface of Area 1 and the ARA result from the same area have been done to discuss similarities and differences. Five locations have been highlighted where similar patterns can be seen in between the two data sets (fig. 5.2.1A and B). These locations are presented below.

Before the comparison is presented it should be stated that the data from the subbottom profiler and from the multibeam sonar are not covering identical areas. Mainly this is due to the fact that the acoustic units are gridded while the ARA is not. Also, the two instruments collecting the data were run separately and do not follow the same survey lines.

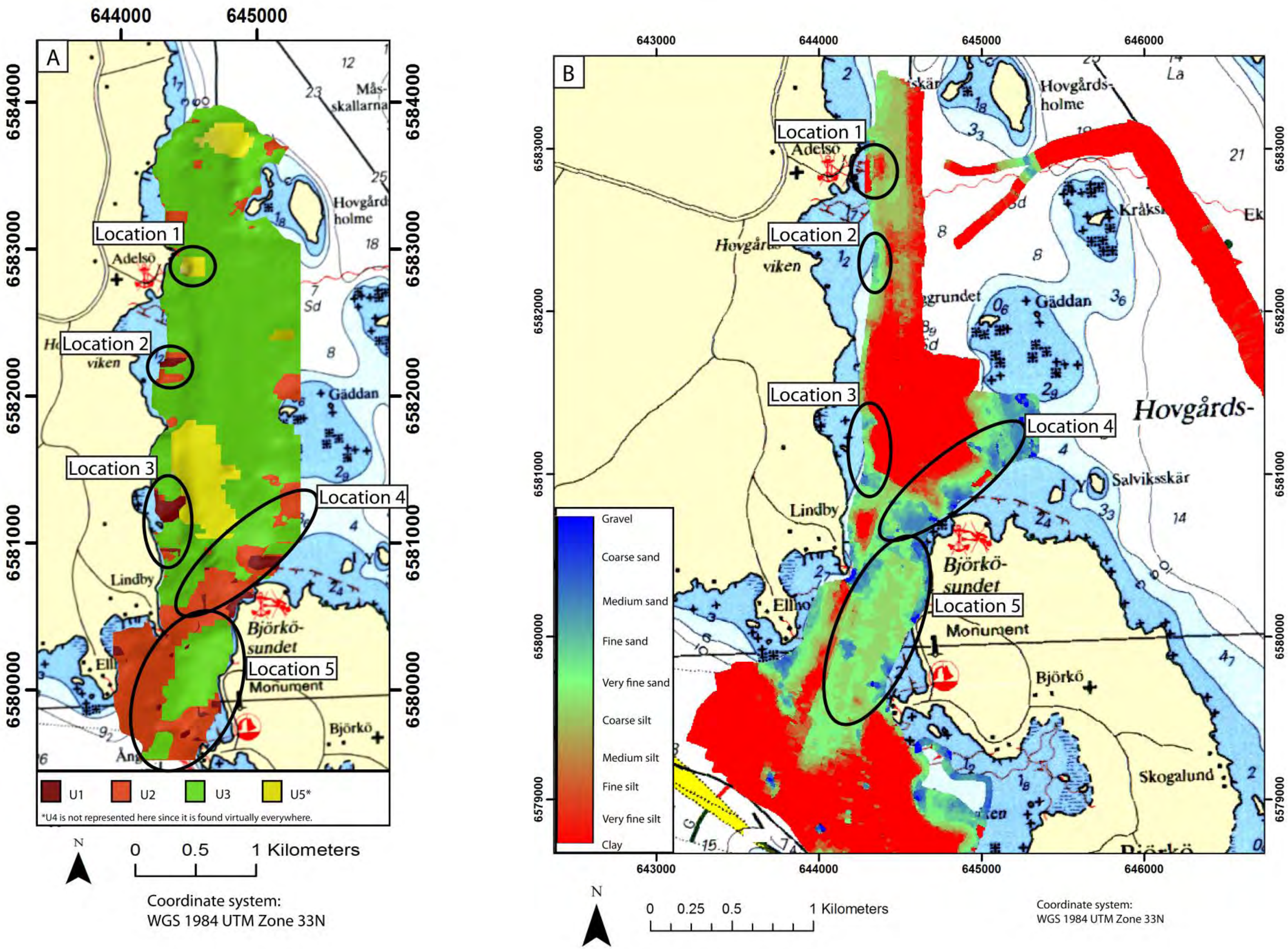

Figure 5.2.1. Comparison in between the distribution of the acoustic sediment units exposed at the lake floor (A) and the ARA result (B) covering Area 1. The black ellipses/circles are highlighting five separate locations where comparisons in between the two data sets are possible. These comparisons are presented below. Basemap is from Sjöfartsverket navigational chart: Mälaren – Östra delen.

Comparison of location 1

Location 1 corresponds to the acoustic unit of U5 (yellow in fig. 5.2.1A). This location is also visible in the ARA map (fig 5.2.1B) where it is suggested that the grain size of U5 in location 1 is clay (fig. 5.2.1B).

Comparison of location 2

In figure 6.5.1A, location 2 can be subdivided into two areas containing a combination of the acoustic units U1 and U2. These two subdivisions are separated by U3. In the ARA result, location 2 is significantly reduced due to the already mentioned sources of uncertainties. It is still possible to hint a tiny strip of the grain size “medium sand” where location 2 begins (fig. 5.2.1 B). This grain size might correspond to the two areas containing the acoustic units U1 and U2.

Comparison of location 3

Location 3 consists of two individual units of U1 and U2 that are separated by U3 (fig. 5.2.1 A). Most of this area is located outside the data coverage of the multibeam sonar (fig. 5.2.1B). Therefore it is not possible to make a fair correlation in between the two data sets. However, it is possible to hint two separate units with the grain size silty to medium sand in location 3 (fig. 5.2.1B). This grain size interval is supported by location 2”, which was correlated to a similar ARA interpretation for U1 and U2.

Comparison of location 4

This location mainly highlights a border in between the two acoustic units U2 and U3 (fig. 5.2.1A). In the ARA result this border has a similar shape, where U2 again is indicated to consist of the grain sizes in between fine and medium sand. The grain size of U3 on the other hand is here indicated to vary from clay to very fine sand (fig. 5.2.1B).

Comparison of location 5

This location highlights an elongated area of the acoustic unit U3 (fig. 5.2.1A). In the ARA result this location corresponds to an area of similar dimensions with varying grain size from coarse silt to very fine sand (fig. 5.2.1B).

The comparison of the five locations shows that it is possible to see somewhat of a correlation in between the different acoustic units from the subbottom profiles and the ARA results. U1 and U2 follow a trend that in most cases are backed up by grain sizes varying from silty to sandy. This comparison are supports the theory of the classification of U1 and U2 as glacial clay. U3 shows a relatively good match to grain sizes varying from silty to very fine sand.

Regarding U5, it only shows correlation in the case of “location 1” that fits very well with the grain size of clay in the ARA results. What is concerning is that there is no sign of correlation in the areas covered by the biggest of the U3 and U5 units found from the middle to the northernmost part of Area 1. In the ARA result, the same area is dominated by the grain size of clay, which means that except the cases in "location 1" and "location 4", the ARA does not show any difference between U3 and U5.

The issue above can depend on several factors. First of all, different sediment types with the same grain size will appear in the same way in the ARA. This is because the ARA only tells differences in grain size, but not in sediment type. When it comes to the distribution, the ARA is more accurate than the acoustic units from the subbottom profiler since the latter one are dependent on the gridding method and its settings, which leads to a relatively generalized result.

5.3 Point objects

The water palisade located on the lake bottom outside Björkö (figure 4.2.1, box B) was probably built for defense reasons (Ingelman-Sundberg, 1972). It is evident that the location of the water palisade differs from the point object types identified in this study. This information therefore raises the question if the different point object types actually are anthropogenic or if they are natural objects resting on the bottom. Based on the information presented in the results of this thesis, this topic will be discussed here.

Type 1 point objects

The type 1 point objects were discussed together with the acoustic sediment unit U5, where it was stated that the origin of this point type cannot be verified without further research. Here there are three main hypothesizes for the origin of the type 1 point objects. In the first one it is stated that the type 1 point objects are gas that emits from the lake floor into the water column. The second hypothesis suggests that the type 1 point objects are seaweed growing in a nutrient rich sediment unit. The third hypothesis suggests that the type 1 point objects are manmade.

Type 2 point objects

There is no multibeam coverage from the areas where the type 2 point objects are situated. Naturally, this makes it hard to speculate any further about the origin of this point type. What can be said is that the objects of this type are located relatively sparse from one another offshore Björkö on a depth of approximately 4 meters. The opaque acoustic nature of these objects indicates that they are not gas, but they can of course be other natural objects, like rocks, which would give this kind of opaque acoustic characteristics.

Type 3 point objects

The shape and dimensions of the type 3 point objects are relatively similar to the first point type. From this point of view it is possible that these two point types are of the same origin. What differs in between the type 1 and type 3 are the acoustic characteristics. While type 1 is transparent type 3 is opaque. Because of this difference it is likely that these objects are not of the same origin.

5.4 Multibeam bathymetry and backscatter features

Several types of features were found in the multibeam bathymetry and backscatter data. To make the decision if these features should be examined more carefully in later studies or not will be discussed here. This decision is to some degree facilitated by combining the multibeam bathymetry and the backscatter data together, which gives a better understanding of the different features on the bottom.

ES feature 1 and BS feature 1

ES feature 1 (fig 4.3.3) is here believed to be originating from mass wasting from the steeper part of the bathymetry closer to the shore line. This hypothesis is fully based on the fan-shape of ES feature 1, that broadens out with increasing water depth. This hypothesis is backed up by BS feature 1 (fig. 4.4.3A and B), which is the corresponding backscatter image of the potential mass wasting feature. BS feature 1 possibly indicates that the grain size of the fan is becoming smaller with increased distance from the coastline, since the backscatter values decreases with depth. Figure 4.4.3B is barely visible in the bathymetry data which may indicate that this is the finest particles that due to suspension have traveled furthest from the source of the potential mass wasting. Due to their relatively small dimensions of these particles they are probably hard to detectet in the multibeam bathymetry data.

ES feature 2 and BS feature 2

When comparing ES feature 2 (fig 4.3.4A-D) with its corresponding backscatter data found in BS feature 2 (fig. 4.4.4A-C), it is evident that all the ES objects A, C and D are visible in the backscatter data while B is not. This comparison supports the theory that the latter ES object is a print in the sediment as believed. The other three objects clearly consist of something else than the surrounding sediments. Ground truthing may therefore be of interest here.

ES feature 4 and BS feature 3

Regarding the pointy objects on top of the relatively elevated parts of the bathymetry (fig. 4.3.6A-D) it is evident that these two features can behave in two different ways in the corresponding backscatter data (fig. 4.4.5A and B).

When speculating in the constituents of these objects based on the comparison above, it is likely that the ES object 4C due to its uniformly high backscatter values is a natural bank made of rocks. The rest of the elevated areas presented in figure 4.3.6 show the same backscatter values and are probably also rocks. The pointy objects on top of the latter examples may on the other hand be wood due to their relatively low backscatter values. Naturally, this speculation cannot be verified without ground truthing data. Ground truthing would particularly be of interest in the case of ES feature 4D, where the pointy objects of low backscatter seem to follow a certain pattern (fig. 4.3.6D).

Clear is that even though there is a visual similarity in the multibeam echosounder result in between the different elevated areas and their attached objects on top, the backscatter result indicates differences in their physical properties.

BS feature 4

All the objects that belongs to BS feature 4 (fig. 4.4.6A-D) are situated in the former harbor area of Birka. Geographically, this increases the potential that any of these objects are of archeological value. This area is also a common place for visitors to take their boats to today, which means that objects seen in the backscatter data also can be of modern origin that have been dropped or lost from the boats. This is nothing that can be verified by studying backscatter data. Therefore, ground truthing would be of interest regarding all the objects that belongs to BS feature 4.

5.5 Shipwrecks

As mentioned in the introduction, shipwrecks are important to examine even if they lack archeological value due to degradation of potentially hazardous fuel tanks and cargo storages (Masetti and Calder, 2012). Therefore, the discussion of the shipwrecks will mainly focus on the four unregistered shipwrecks found in the backscatter data.

Shipwreck 2

This shipwreck (fig.4.5.2) is as mentioned unregistered. It is also the only shipwreck in this thesis that exclusively is visible in the multibeam backscatter data but not in the bathymetry data. This may mean that the shipwreck is degraded enough to keep the same level as the bathymetry, which in turn depends on the time that the shipwreck has spent on the bottom together with what kind of material the shipwreck consists of. It is likely that this ship is made of some other, less resistant material than the majority of the other shipwrecks found in this area that in most of the cases are modern barge vessels. Chances are therefore relatively high that shipwreck 2 consists of wood. A wooden ship is a postulate if it by any chances would be a Viking ship. Therefore further research is suggested here.

Shipwreck 4

This shipwreck (fig. 4.5.4) is as mentioned not registered but has been confirmed and reported before (Flood, personal communication). It is therefore suggested to include this shipwreck in the Fornsök register.

Shipwreck 5X

The unregistered shipwreck 5X is either placed below or above the registered shipwreck 5 (figs. 4.5.5 and 4.6.1). If it is placed below it was probably not spotted during the registration of shipwreck 5. If it is placed above it may have sunk after the registration. Both the wrecks in this case look like modern barge vessels. It is suggested that it should be clear in the Fornsök register which one is which and to register the one that is not in Fornsök at the moment.

Shipwreck 11

The previously unknown shipwreck 11 (figs. 4.5.9 and 4.6.2) is of interest from an archeological point of view since its dimensions (13×3 m) reminds of the ship "Skuldelev 3" (14×3 m) from the 11^{th} century (Lidén, personal communication). This wreck would therefore be interesting to examine closer, even if the 3D model of shipwreck 11 (fig. 4.6.2) reminds of a modern speed boat.

Shipwreck 12

Shipwreck 12 (figs. 4.5.10 and 4.6.3) seems to have had a cargo leak from its hull. This suggestion is based on the area that reaches about 10 meters to the south of the wreck with the significantly higher backscatter values compared to its surroundings. This area seems to originate from the shipwreck. In this case it is confirmed that the actual ship was shipping sand before it sank (Fornsök, 2012-10-04), which supports the cargo leak hypothesis since the ARA analysis from the potential leak indicates a grain size of sand to gravel in the otherwise clay dominated bottom sediment.

6. Conclusion

The first of the two main aims of this thesis was to interpret the sediment stratigraphy of the Björkö strait and calculate the volume of the black soil.

The acoustic sediment stratigraphy of the study area was divided into five individual acoustic units (U1-U5). Most of these units are influenced by the stages of the Baltic Sea basin (U1-U3). U4 and U5 are probably formed after the isolation of Lake Mälaren (1000-1300 AD) (Risberg et al., 2002). The distribution of the interpreted acoustic units exposed at the lake floor are partly supported by the ARA result, which occasionally shows a good fit in between the grain size distribution and the previously mentioned acoustic acoustic units. The black soil unit could not be visualized in the data set underlying this thesis.

The second of the two main aims of this thesis was to produce bathymetric and backscatter maps where objects were located with the primary focus to find archeological artifacts from the Vikings of Birka.

Several types of objects were characterized in the bathymetry and the backscatter data. These objects may be of archeological value but need to be confirmed through ground truthing data. Here it is suggested that the following objects should be further examined:

- Shipwreck 2 (fig. 4.5.2) due to its relatively degraded condition which may indicate it has an age of archeological value.
- Shipwreck 11 (figs. 4.5.9 and 4.6.2) due to its different dimensions compared to the majority of the registered shipwrecks in this area.
- The backscatter features in figure 4.4.4 and figure 4.4.6 due to their geographical locations in the Björkö strait.
- The relatively shallow areas with pointy objects on top should be further investigated (fig. 4.3.6A-D). This is due to the fact that the backscatter result tells that the majority of these areas are not naturally banks consisting of rocks, but something else (fig. 4.4.5A-B).
- The type 1 point objects from the acoustic subbottom data are also suggested to be included in a detailed study. This is because of their geographical location in the Björkö strait together with the relatively even spacing in between four of these objects (fig. 4.2.1 box A).

In addition to the geological value, this type of study could therefore be of a significant value for marine archeological investigations where the environment and the human impact are merged.

7. References

Andrén, E., Andrén, T., Sohlenius, G., 2000. The Holocene history of the southwestern Baltic Sea as reflected in a sediment core from the Bornholm Basin. Boreas 29, 233 - 250.

Andrén, T., Björck, S., Andrén, E., Conley, D. J., Lambeck, K., Zillén, L., 2011. The development of the Baltic Sea basin during the last 130 000 years. *In* The Baltic Sea Basin, Springer Berlin/Heidelberg, 75-97.

Bellec, V., Wilson, M., Böe, R., Rise, L., Thorsnes, T., Buhl-Mortensen, L., Buhl-Mortensen, P., 2007. Bottom currents interpreted from iceberg ploughmarks revealed by multibeam data at Tromsöflaket, Barents Sea. Marine Geology, 249:257-270.

Björck, S., 1995. A review of the history of the Baltic Sea, 13.0-8.0 ka BP. Quaternary International 27, 19-40.

Björck, S., 2011. The late Quaternary development of the Baltic Sea. In The Baltic Sea Basin, Springer Berlin/Heidelberg,

Björck, S., Kromer, B., Johnsen, S., Bennike, O., Hammarlund, D., Lemdahl, G., Possnert, G., Rasmussen, T.L., Wohlfarth, B., Hammer, C.U., Spurk, M., 1996. Synchronized Terrestrial-Atmospheric Deglacial Records Around the North Atlantic. Science, 274:1155-1160.

Brunnberg, L., 1988. Diatoms in glacial clay in the Södertörn area, Stockholm region. In: Miller, U. and Robertsson, A-M,. (eds), Proceedings of Nordic Diatomist Meeting. University of Stockholm, Department of Quaternary Research Report, 12, 7-9.

Burrough, P.A., McDonnell, A., 2009. Optimal Interpolation Using Geostatistics, in Principles of Geographical Information Systems: Spatial Information Systems and Geostatistics. Oxford University Press, Great Britain, 132-134.

Canet, C., Prol-Ledesma, R.M., Dando, P.R., Figueroa, V., Shumilin, E., Birosta, E., Sanchez, A., Robinson, C.J., Camprubi, A., Tauler, E., 2010. Discovery of massive seafloor gas seepage along the Wagner Fault, northern Gulf of California. Sedimentary Geology, 228:292-303.

de Geer., 2002. Geochronology of the last 12,000 years. Geol Rundsch, 3:457-471.

Flodén, T., Söderberg, P., Wickman, F.E., 1993. Björkö, a possible Middle Proterozoic impact structure of Stockholm, Sweden. Geologiska Föreningens I Stockholm Förhandlingar, 115:25-38.

Fonseca, L., Brown, C., Calder, B., Mayer, L., Rzhanov, Y., 2008. Angular range analysis of acoustic themes from Stanton Banks Ireland: A link between visual interpretation and multibeam echosounder angular signatures. Applied Acoustics, 90:1298-1304.

Fonseca, L., Mayer, L., 2007. Remote estimation of surficial seafloor properties through the application Angular Range Analysis to multibeam sonar data. Marine Geophysical Researches, 28:119-126.

Hamilton, L.J., Parnum, I., 2011. Acoustic seabed segmentation from direct statistical clustering of entire multibeam sonar backscatter curves. Continental Shelf Research, 31:138-148.

Harrison, D., 2009, *Sveriges historia 600-1350,* Nordstedts, Stockholm, 342 p.

Hell, B., 2011. Mapping bathymetry - From measurements to applications, Doctoral thesis in marine geosciences, Department of Geological Sciences, Stockholm University.

Holmquist-Olausson, L., 2002. Patterns of settlement and defence at the Proto-town of Birka, Lake Mälaren, Eastern Sweden. The Scandinavians from the Vendel Period to the tenth century. An etnographic Perspective. J. Jesch (ed.) San Marino.

Hovland, M., 2007. Discovery of prolific natural methane seeps at Gullfaks, northern North Sea. Geo-Marine Letters, 27:197-201.

Hutri, K-L., Kotilainen, A., 2007. An acoustic view into Holocene palaeoseismicity offshore southwestern Finland, Baltic Sea. Marine Geology, 238:45-59.

Ignatius, H., 1958. On the rate of sedimentation in the Baltic Sea. Bulletin Commision Géologique Finlande, 180, 135-145.

Ignatius, H., Axberg, S., Niemistö, L., Winterhalter, B., 1981. Quaternary geology of the Baltic Sea. In: Voipio, A. (Ed.), The Baltic Sea, Elsevier, Amsterdam, ?:54-104.

Ingelman-Sundberg, C., 1972. Undervattensarkeologisk undersökning utanför Birka. Fornvännen 67, 127-135.

Le Bas, T.P., Huvenne, V.A.I., 2009. Acquisition and processing of backscatter data for habitat mapping – Comparison of multibeam and sidescan systems. Applied Acoustics, 70:1248-1257.

Lundqvist, J., 2004. Glacial history of Sweden. Developments in Quaternary Sciences, 2:285-311.

Mallace, D., Gee, L., 2005. Multibeam processing – the end to manual editing? The Hydrographic Society of America, Conference proceedings.

Masetti, G., Calder, B., 2012. Remote identification of a shipwreck site from MBES backscatter. Journal of Environmental Management, 111:44-52.

Penrose, J.D., Siwabessy, P.J.W., Gavrilov, A., Parnum, I., Hamilton, L.J., Bickers, A., Brooke, B., Ryan, D.A., Kennedy, P., 2005. Acoustic Techniques for Seabed Classification. Cooperative Research Centre for Coastal Zone Estuary and Waterway Management, Technical report 32.

Reitdorf, A., Daub, C., Loef, P., 2006. Precise positioning in Real-Time using Navigation Satellites and Telecommunication. Proceedings of the 3rd workshop on positioning, navigation and communication, (WPNC'06).

Risberg, J., Björck, J., 1997. Lithostratigraphy in the Björkö Strait, Lake Mälaren. In Miller, U., Clarke, H., Hansson, A-M., Johansson, B.M., Ambrosiani, B., Hackens, T., (eds). Environment and Vikings. PACT 52, 249-260.

Risberg, J., Karlsson, S., Hansson, A-H., Hedenström, A., Heimdahl, J., Miller, U., Tingvall, C., 2002. Environmental changes and human impact as recorded in a sediment sequence offshore from a Viking Age town, Birka, southeastern Sweden. The Holocene, 12:445

Rzhanov, Y., Fonseca, L., Mayer, L., 2011. Construction of seafloor thematic maps from multibeam acoustic backscatter angular response data. Computers & Geosciences, 41:181-187.

Santamarina, J.C., Rinaldi, V.A., Fratta, D., Klein, K.A., Wang, Y-H., Cho, G-C., Cascante, G., 2005. A survey of elastic and electromagnetic properties of near-surface soils. D. Buttler (Ed.), Near-Surface Geophysics, p. 71-87

Svensson, E., 2010. Potential Shipwreck Pollution in the Baltic Sea. Overview of Work in the Baltic Sea States, supplementary report ed. Swedish Maritime Administration and Lighthouse, Norrköping (Sweden).

von Deimling, J.S., Papenberg, C., 2012. Technical Note: Detection of gas bubble leakage via correlation o water column multibeam images. Ocean Science, 8:175-181.

Internet sources

Jakobsson, M., 2012a. Sonar application and signal processing. *In* Marine Geoscientific Research Methods HT12, Department of Geological Sciences, Stockholm.

http://www.geo.su.se/images/file_archive/marine_geosci_res_meth/HT12/marinegeophysical methods-processing-2012.pdf

Jakobsson, M., 2012b. Multibeam and side scan mapping. *In* Marine Geoscientific Research Methods HT12, Department of Geological Sciences, Stockholm.

http://www.geo.su.se/images/file_archive/marine_geosci_res_meth/HT12/marinegeophysical-multibeam-2012.pdf

Kongsberg Maritime AS, 2010. MRU 5+ - The ultimate marine motion sensor.

http://www.km.kongsberg.com/ks/web/nokbg0397.nsf/AllWeb/A835CAA3D6E43C6BC12575AE004AA55B/$file/Datasheet_mru5plus_okt10.pdf

Kongsberg Maritime AS, 2012. EM2040 Multibeam echo sounder – True wide band high resolution multibeam echo sounder.

http://www.km.kongsberg.com/ks/web/nokbg0397.nsf/AllWeb/248996D7F1021D46C12575E500285652/$file/332644_em2040_product_specification.pdf?OpenElement

Maringeologiska kartan Mälaren.

http://www.sgu.se/sgu/sv/produkter-tjanster/produkter/sgu_publ/publ_beskr/K223.html, Sveriges Geologiska Undersökning, retrieved 2012-05-08

Mälaren.

http://www04.sub.su.se:2070/lang/mälaren,

Nationalencyklopedin, retrieved 2012-05-08

Swedish national heritage board – Riksantikvarieämbetet, Fornsök.

RAÄ numbers: Adelsö 188, Ekerö 243, Ekerö 235, Ekerö 247, Ekerö 228, Ekerö 231, Ekerö 232, Ekerö 225 and Ekerö 208.

http://www.fmis.raa.se/cocoon/fornsok/search.html

8. Appendix

8.1 Surfer gridding reports

The key parameters and their individual settings used to grid each acoustic unit found in the figures 4.2.6 and 4.2.7 are presented here. Some of these settings vary depending on the actual sediment unit and if the unit belongs to Area 1 or Area 2. The details are found below.

U1 Area 1

Gridding Rules

Gridding Method:	Kriging
Kriging Type:	Point

Search Parameters

Search Ellipse Radius #1:	200
Search Ellipse Radius #2:	50
Search Ellipse Angle:	0
Number of Search Sectors:	4
Maximum Data Per Sector:	16
Maximum Empty Sectors:	3
Minimum Data:	8
Maximum Data:	64

Output Grid

Grid Size:	100 rows x 30 columns
Total Nodes:	3000
Filled Nodes:	2009
Blanked Nodes:	991
Blank Value:	1.70141E+038

Grid Geometry

X Minimum:	643835.975
X Maximum:	645155.099
X Spacing:	45.487034482761 m
Y Minimum:	6579527.871
Y Maximum:	6584031.0874138
Y Spacing:	45.487034482722 m

U2 Area 1

Gridding Rules

Gridding Method:	Kriging
Kriging Type:	Point

Search Parameters

Search Ellipse Radius #1:	200
Search Ellipse Radius #2:	50
Search Ellipse Angle:	0
Number of Search Sectors:	4
Maximum Data Per Sector:	16
Maximum Empty Sectors:	3
Minimum Data:	8
Maximum Data:	64

Output Grid

Grid Size:	100 rows x 30 columns
Total Nodes:	3000
Filled Nodes:	1992
Blanked Nodes:	1008
Blank Value:	1.70141E+038

Grid Geometry

X Minimum:	643835.975
X Maximum:	645155.099
X Spacing:	45.487034482761 m
Y Minimum:	6579527.871
Y Maximum:	6584031.0874138
Y Spacing:	45.487034482722 m

U3 Area 1

Gridding Rules

Gridding Method:	Kriging
Kriging Type:	Point

Search Parameters

Search Ellipse Radius #1:	200
Search Ellipse Radius #2:	50
Search Ellipse Angle:	0
Number of Search Sectors:	4
Maximum Data Per Sector:	16
Maximum Empty Sectors:	3
Minimum Data:	8
Maximum Data:	64

Output Grid

Grid Size:	100 rows x 25 columns
Total Nodes:	2500
Filled Nodes:	1732
Blanked Nodes:	768
Blank Value:	1.70141E+038

Grid Geometry

X Minimum:	644056.503
X Maximum:	645155.099
X Spacing:	45.774833333334 m
Y Minimum:	6579531.898
Y Maximum:	6584063.6065
Y Spacing:	45.77483333333 m

U5 Area 1

Gridding Rules

Gridding Method:	Kriging
Kriging Type:	Point

Search Parameters

Search Ellipse Radius #1:	200
Search Ellipse Radius #2:	50
Search Ellipse Angle:	0
Number of Search Sectors:	4
Maximum Data Per Sector:	16
Maximum Empty Sectors:	3
Minimum Data:	30
Maximum Data:	64

Output Grid

Grid Size:	100 rows x 26 columns
Total Nodes:	2600
Filled Nodes:	348
Blanked Nodes:	2252
Blank Value:	1.70141E+038

Grid Geometry

X Minimum:	644223.194
X Maximum:	645077.883
X Spacing:	34.187560000001 m
Y Minimum:	6580700.564
Y Maximum:	6584085.13244
Y Spacing:	34.187559999996 m

U1 Area 2

Gridding Rules

Gridding Method:	Kriging
Kriging Type:	Point

Search Parameters

Search Ellipse Radius #1:	200
Search Ellipse Radius #2:	50
Search Ellipse Angle:	0
Number of Search Sectors:	4
Maximum Data Per Sector:	16
Maximum Empty Sectors:	3
Minimum Data:	8
Maximum Data:	64

Output Grid

Grid Size:	100 rows x 84 columns
Total Nodes:	8400
Filled Nodes:	1331
Blanked Nodes:	7069
Blank Value:	1.70141E+038

Grid Geometry

X Minimum:	644359.471
X Maximum:	650676.59596937
X Spacing:	76.10993939 m
Y Minimum:	6575588.218
Y Maximum:	6583123.102
Y Spacing:	76.109939393935 m

U2 Area 2

Gridding Rules

Gridding Method:	Kriging
Kriging Type:	Point

Search Parameters

Search Ellipse Radius #1:	200
Search Ellipse Radius #2:	50
Search Ellipse Angle:	0
Number of Search Sectors:	4
Maximum Data Per Sector:	16
Maximum Empty Sectors:	3
Minimum Data:	8
Maximum Data:	64

Output Grid

Grid Size:	100 rows x 82 columns
Total Nodes:	8200
Filled Nodes:	1261
Blanked Nodes:	6939
Blank Value:	1.70141E+038

Grid Geometry

X Minimum:	644360.925
X Maximum:	650487.07527285
X Spacing:	75.631484849999 m
Y Minimum:	6575635.585
Y Maximum:	6583123.102
Y Spacing:	75.631484848485 m

U3 Area 2

Gridding Rules

Gridding Method:	Kriging
Kriging Type:	Point

Search Parameters

Search Ellipse Radius #1:	200
Search Ellipse Radius #2:	50
Search Ellipse Angle:	0
Number of Search Sectors:	4
Maximum Data Per Sector:	16
Maximum Empty Sectors:	3
Minimum Data:	8
Maximum Data:	64

Output Grid

Grid Size:	100 rows x 83 columns
Total Nodes:	8300
Filled Nodes:	950
Blanked Nodes:	7350
Blank Value:	1.70141E+038

Grid Geometry

X Minimum:	644418.849
X Maximum:	650659.86402998
X Spacing:	76.10993939 m
Y Minimum:	6575588.218
Y Maximum:	6583123.102
Y Spacing:	76.109939393935 m

8.2 Coordinates for the objects of interest

The table 8.2.1 A-B lists all the objects of interest together with their respective figure numbers and coordinates (WGS 84 UTM zone 33 N). The type 1 point objects highlighted in blue (table 8.2.1A) are situated with relatively even spacing in between each other on a straight line (fig. 4.3.1 box A).

Acoustic subbottom objects

Point type 1	Northing	Easting		Figure in thesis
1	6581120	644371		4.3.1 box A
2	6581329	644385		4.3.1 box A
3	6581477	644430		4.3.1 box A
4	6581671	644458		4.3.1 box A
5	6581357	644357		4.3.1
6	6581436	644325		4.3.1
7	6582045	644664		4.3.1
8	6583849	644415		4.3.1
9	6581405	644859		4.3.1
10	6581447	644859		4.3.1
11	6580333	644437		4.3.1
12	6580792	645874		4.3.1
13	6576801	646684		4.3.1
Point type 2	**Northing**	**Easting**		
1	6581420	644334		4.3.1
2	6581344	644326		4.3.1
3	6580410	646020		4.3.1
4	6579290	647038		4.3.1
5	6577335	645978		4.3.1
6	6577442	645711		4.3.1
7	6577451	645663		4.3.1
8	6578672	644886		4.3.1
Point type 3	**Northing**	**Easting**		
1	6578517	644851		4.3.1
2	6578671	644885		4.3.1

Table 8.2.1A. The coordinates for all the point objects that were registered with the acoustic subbottom profiler. All these point objects are placed in relation to each other in figure 4.3.1. The four objects that are highlighted in blue are situated with relatively even spacing in between each other (fig. 4.3.1 box A).

Multibeam objects

ES feature 4	Northing	Easting		Figure in thesis
A	6581163	644958		4.3.6A
B	6580352	644215		4.3.6B
D	6579005	644606		4.3.6D
BS feature 2	**Northing**	**Easting**		
A	6581715	644309		4.4.4A
B	6581681	644311		4.4.4B
C	6581562	644297		4.4.4C
BS feature 4	**Northing**	**Easting**		**Figure**
A: circular	6580133	644586		4.4.6A
A: elongated	6580128	644582		4.4.6A
B	6580148	644548		4.4.6B
C	6580191	644617		4.4.6C
D: longer	6580344	644651		4.4.6D
D: shorter	6580328	644664		4.4.6D
Shipwreck no.	**Northing**	**Easting**		**Figure**
2	6577525	647697		4.5.2
5	6576745	648504		4.5.5 and 4.6.1
5X	6576745	648504		4.5.5 and 4.6.1
11	6575347	649473		4.5.9 and 4.6.2

Table 8.2.1B. The coordinates for all the objects of interest that were registered with the multibeam sonar.